NTIRE 2024 Challenge on Low Light Image Enhancement: Methods and Results

Xiaoning Liu* Zongwei Wu* Ao Li* Florin-Alexandru Vasluianu* Yulun Zhang*
Shuhang Gu* Le Zhang* Ce Zhu* Radu Timofte* Zhi Jin Hongjun Wu
Chenxi Wang Haitao Ling Yuanhao Cai Hao Bian Yuxin Zheng Jing Lin
Alan Yuille Ben Shao Jin Guo Tianli Liu Mohao Wu Yixu Feng Shuo Hou
Haotian Lin Yu Zhu Peng Wu Wei Dong Jinqiu Sun Yanning Zhang
Qingsen Yan Wenbin Zou Weipeng Yang Yunxiang Li Qiaomu Wei Tian Ye
Sixiang Chen Zhao Zhang Suiyi Zhao Bo Wang Yan Luo Zhichao Zuo
Mingshen Wang Junhu Wang Yanyan Wei Xiaopeng Sun Yu Gao
Jiancheng Huang Hongming Chen Xiang Chen Hui Tang Yuanbin Chen
Yuanbo Zhou Xinwei Dai Xintao Qiu Wei Deng Qinquan Gao Tong Tong
Mingjia Li Jin Hu Xinyu He Xiaojie Guo Sabarinathan K Uma
A Sasithradevi B Sathya Bama S. Mohamed Mansoor Roomi V.Srivatsav
Jinjuan Wang Long Sun Qiuying Chen Jiahong Shao Yizhi Zhang
Marcos V. Conde Daniel Feijoo Juan C. Benito Alvaro García Jaeho Lee
Seongwan Kim Sharif S M A Nodirkhuja Khujaev Roman Tsoy Ali Murtaza
Uswah Khairuddin Ahmad ’Athif Mohd Faudzi Sampada Malagi Amogh Joshi
Nikhil Akalwadi Chaitra Desai Ramesh Ashok Tabib Uma Mudenagudi
Wenyi Lian Wenjing Lian Jagadeesh Kalyanshetti Vijayalaxmi Ashok Aralikatti
Palani Yashaswini Nitish Upasi Dikshit Hegde Ujwala Patil Sujata C
Xingzhuo Yan Wei Hao Minghan Fu Pooja choksy Anjali Sarvaiya
Kishor Upla Kiran Raja Hailong Yan Yunkai Zhang Baiang Li Jingyi Zhang
Huan Zheng

Abstract

This paper reviews the NTIRE 2024 low light image enhancement challenge, highlighting the proposed solutions and results. The aim of this challenge is to discover an effective network design or solution capable of generating brighter, clearer, and visually appealing results when dealing with a variety of conditions, including ultra-high resolution (4K and beyond), non-uniform illumination, backlighting, extreme darkness, and night scenes. A notable total of 428 participants registered for the challenge, with 22 teams ultimately making valid submissions. This paper meticulously evaluates the state-of-the-art advancements in enhancing low-light images, reflecting the significant progress and creativity in this field.

1. Introduction

Low light Image enhancement (LLIE), a pivotal yet challenging task in computer vision, aims to improve visibility and contrast across a broad spectrum of low-light scenarios, including uneven illumination, extreme darkness, backlighting, and night. Additionally, LLIE strives to correct imperfections like noise, artifacts, and color distortion. These challenges, arising in darkness or through illumination enhancement, affect both human visual perception and downstream tasks like object detection and scene segmentation.

As deep learning technology improves by leaps and bounds, remarkable advances in LLIE are impressive. However, current cutting-edge methods [8, 34, 39, 47, 55, 72, 78] not only struggle to adapt to complex and variable low-light conditions but also face major challenges when being deployed on consumer-grade devices such as smartphones and

* X. Liu, Z. Wu, A. Li, F. Vasluianu, Y. Zhang, S. Gu, L. Zhang, C. Zhu and R. Timofte were the challenge organizers, while the other authors participated in the challenge. Each team described their own method in the report. Appendix A contains the authors' teams and affiliations.
NTIRE 2024 webpage: https://cvlai.net/ntire/2024.
Code: https://github.com/AVC2-UESTC/NTIRE24-LLE/

cameras. This is primarily constrained by the limitations of current datasets [7, 71] that suffer from limited scene diversity (notably insufficient night scenes), low resolution, and overly simplistic lighting conditions. Additionally, the high complexity of models [8, 38, 39, 69, 74] hampers their ability to handle ultra-high resolution images that are commonly captured by smartphones.

To address the aforementioned challenges, we launched the inaugural Low Light Enhancement Challenge at the 2024 New Trends in Image Restoration and Enhancement (NTIRE 2024) workshop. The objective of this challenge is to foster innovative thinking and discover solutions that significantly improve image quality under various low-light conditions. To this end, we have built an LLIE dataset that features a wide range of scenes, encompassing various low-light conditions. These images include indoor and outdoor locations under both daylight and nighttime conditions, with the challenge focusing on enhancing image quality across these diverse settings.

In conclusion, this challenge aims to set a new benchmark for LLIE while highlighting specific challenges and research questions in this domain. We hope that it will inspire the research community to explore these pressing issues and identify emerging trends. Moreover, this challenge is one of the NTIRE 2024 Workshop associated challenges on: dense and non-homogeneous dehazing [1], night photography rendering [4], blind compressed image enhancement [73], shadow removal [67], efficient super resolution [64], image super resolution (×4) [20], light field image super-resolution [70], stereo image super-resolution [68], HR depth from images of specular and transparent surfaces [77], bracketing image restoration and enhancement [81], portrait quality assessment [17], quality assessment for AI-generated content [48], restore any image model (RAIM) in the wild [45], RAW image super-resolution [24], short-form UGC video quality assessment [44], low light enhancement [49], and RAW burst alignment and ISP challenge.

2. NTIRE 2024 Low Light Enhancement Challenge

The objectives of this challenge are threefold: (1) to advance research in the field of low light enhancement, (2) to facilitate systematic comparisons among different methodologies, and (3) to provide a forum for both academic and industrial stakeholders to interact, deliberate, and potentially forge partnerships. This section delves into the detailed aspects of the challenge.

2.1. Dataset

Although some low light datasets, such as LOL [71] and MIT-Adobe FiveK [7], have been widely applied in the field, they exhibit limitations previously mentioned, including limited resolution, monotonous scene content, and uniform illumination levels. These factors often restrict the generalization capabilities of cutting-edge models [8, 39, 47, 55, 72, 78], posing significant challenges in adapting to diverse low-light conditions, especially when implemented on consumer-grade devices like smartphones and cameras. To address these issues, this challenge introduces a rich array of contest scenarios, covering a variety of lighting conditions such as dim environments, extreme darkness, non-uniform illumination, backlighting, and night scenes, applicable to both indoor and outdoor settings during day and night, with image resolutions up to 4K and beyond. Specifically, the dataset includes 230 training scenes, along with 35 validation and 35 testing scenes. The ground truth (GT) images for both validation and testing were kept concealed from the participants throughout the challenge. Further details about the dataset will be provided in subsequent works.

2.2. Tracks and Competition

Ranking statistic. In this challenge, we primarily use peak signal-to-noise ratio (PSNR), structural similarity (SSIM), and Learned Perceptual Image Patch Similarity (LPIPS) [80] as the criteria for comparing models submitted by participants. Given that LPIPS is a learned perceptual evaluation metric and our competition focuses mainly on quantitative assessments, We use LPIPS as a supplementary evaluation tool when the quantitative evaluations of two methods are indistinguishable. As listed in Tab. 1, "Final Rank" represents a composite metric, calculated through a weighted sum of PSNR (60%) and SSIM (40%). This way offers a comprehensive evaluation of the effectiveness of each solution in enhancing low-light conditions.

Challenge phases. *(1) Development and validation phase*: Participants were granted access to 230 training image pairs and 35 validation inputs from our constructed dataset. It is noteworthy that the GT images for the validation set were hidden from the participants. Participants had the opportunity to submit their enhanced results to the evaluation server, which calculated the PSNR and SSIM for the enhanced images generated by their models and provided immediate feedback. *(2) Testing phase:* Participants gained access to 35 testing low light images from the built dataset, with the ground-truth images remaining undisclosed. Submissions of their enhanced outputs were made to the Codalab evaluation server, accompanied by an email to the organizers containing the code and a factsheet. The organizers subsequently verified and executed the provided code to derive the final results, which were shared with participants upon the conclusion of the challenge.

Table 1. Evaluation and Rankings in the NTIRE 2024 Low Light Enhancement Challenge. This table presents a comprehensive comparison of participant solutions across multiple metrics: PSNR, SSIM, and LPIPS. “Rank PSNR” and “Rank SSIM” indicate the respective standings of participants based on their performance in PSNR and SSIM metrics on the challenge’s test dataset. “Final Rank” represents a composite metric, derived from a weighted sum of PSNR (60%) and SSIM (40%), which provides an overall assessment of each solution’s effectiveness in low light enhancement.

Team	PSNR	SSIM	LPIPS	Rank PSNR	Rank SSIM	Final Rank
SYSU-FVL-T2	25.52	0.8637	0.1221	1	1	1
Retinexformer [8]	25.30	0.8525	0.1424	2	4	2
DH-AISP	24.97	0.8528	0.1235	3	3	3
NWPU-DiffLight	24.78	0.8556	0.1673	6	2	4
GiantPandaCV	24.83	0.8474	0.1353	5	7	5
LVGroup_HFUT	24.88	0.8395	0.1371	4	10	6
Try1try8	24.49	0.8483	0.1359	8	6	7
Pixel_warrior	24.74	0.8416	0.1514	7	9	8
HuiT	24.13	0.8484	0.1436	10	5	9
X-LIME	24.28	0.8446	0.1298	9	8	10
Image Lab	23.63	0.8235	0.1673	11	12	11
dgzzqteam	23.28	0.8385	0.1406	12	11	12
Cidaut AI (InstructIR [23])	23.07	0.8075	0.1559	13	16	13
OptDev	22.93	0.8097	0.1592	14	15	14
ataza	22.51	0.8161	0.1404	18	13	15
KLETech-CEVI_LowlightHypnotise	22.85	0.7828	0.1823	15	18	16
221B	22.04	0.8141	0.1084	19	14	17
KLETech-CEVI_Dark_Knights	22.76	0.7843	0.1806	17	17	18
BFU-LL	22.78	0.7792	0.1826	16	19	19
SVNIT_NTNU	20.32	0.7718	0.3089	20	20	20
yanhailong	20.07	0.6881	0.3133	21	22	21
Mishka	18.19	0.7161	0.2712	22	21	22

3. Challenge Results and Discussion

The results of the low light enhancement challenge are detailed in Tab. 1, which evaluates and ranks the performances of 22 teams. Notably, one team, AiRiA_Vision, voluntarily withdrew from the ranking due to issues related to their model design. The evaluation leverages two key performance metrics: PSNR and SSIM. The metrics are calculated based on a test set comprising 35 inputs from the built dataset, thereby ensuring the challenge’s integrity and mitigating the risk of overfitting to the validation set.

The top-ranked teams in the challenge boast higher PSNR and SSIM values, signifying superior performance, while the lower-ranked teams exhibit lower values, indicative of suboptimal performance. Notably, two teams achieved a PSNR of over 25 dB, meeting our prior expectations for this metric. For more detailed information on the low-light enhancement methods employed, please refer to Sec. 4, which discusses the specific solutions provided by each team.

Due to the ultra-high resolution (4K and beyond) of the input images, many teams opted for multi-scale strategies to implement enhancement. While they has indeed reduced computational consumption to some extent, currently, almost all models are unable to perform inference on a plain GPU, *e.g.* , one with 12G memory. For the next competition, we will consider including NIQE [59] along with metrics measuring model efficiency, such as inference time, model parameter count, computational complexity (FLOPs), and memory consumption. This will promote the application of ultra-high-resolution low light enhancement on smartphones.

4. Challenge Methods and Teams

4.1. SYSU-FVL-T2

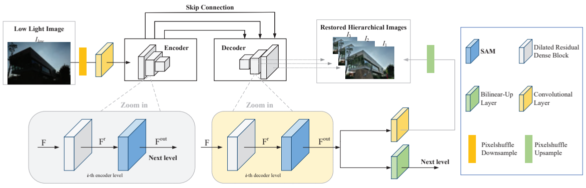

Figure 1. The backbone network employed in our method. (Reproduced from ESDNet [75])

Description: As shown in Fig. 1, ESDNet-L [75] is employed as the backbone in our proposed method for low-light image enhancement. The backbone mainly consists of an encoder-decoder network in three feature scales with skip-connections. Different scales of features are generated by adopting the bilinear interpolation. In each scale, the Semantic-Aligned Scale-Aware Modules (SAM) are stacked to enhance the ability of the model to address scale variations. SAM incorporates a pyramid context extraction module and a cross-scale dynamic fusion module to selectively fuse multi-scale features.

Furthermore, for network training, the loss function L_{total} is set for outputs in three scales $\hat{I}_1, \hat{I}_2, \hat{I}_3$:

$$L_{total} = \sum_{i=1}^{3} L_C\left(I_i, \hat{I}_i\right) + \lambda \cdot L_P\left(I_i, \hat{I}_i\right), \tag{1}$$

where λ is set as 0.04, I_i stands for ground truth image, $\hat{I}_i$ stands for enhanced image, L_C stands for Charbonnier loss [42], and L_P stands for perceptual loss using pretrained VGG19 model [66].

Implementation: The proposed method is based on Python 3.8 and the experiment is conducted on one NVIDIA RTX A6000 GPU (49G). Inspired by MIRNet-v2 [79], we adopt a progressive training strategy. The model is trained for 150000 iterations from scratch and optimized by Adam [41]. During the training process, at the first stage, the batch size is set to 8, and we randomly crop square image patches of size 720 for training. Subsequently, after 46000, 32000, 24000, 18000, and 18000 iterations, the batch size decreases to 4, 4, 2, 2, and 1, respectively. The lengths of the square image patches are set to 1024, 1024, 1280, 1280, and 1600 for the respective stages. The learning rate is set as 2×10^{-4} initially and is scheduled by cyclic cosine annealing [52]. During the testing phase, the whole low-light image is fed into the network, and the enhanced image is obtained directly. The batchsize in testing is set as 1.

4.2. Retinexformer

The proposed code, pre-trained models, results, and training logs are all publicly available at https://github.com/caiyuanhao1998/Retinexformer.

Description: The team directly adopt their ICCV 2023 work Retinexformer [8] to participate this challenge. Fig. 2 illustrates the overall architecture of their method. As shown in Fig. 2 (a), Retinexformer is based on their formulated One-stage Retinex-based Framework (ORF). Their Retinexformer takes a low-light image $\mathbf{I} \in \mathbb{R}^{H\times W\times 3}$ as input and reconstruct its enhanced counterpart $\mathbf{I}_{en} \in \mathbb{R}^{H\times W\times 3}$. The original Retinex model assumes that the low-light image $\mathbf{I}$ is corruption-free and can be decomposed into a reflectance image $\mathbf{R} \in \mathbb{R}^{H\times W\times 3}$ and an illumination map $\mathbf{L} \in \mathbb{R}^{H\times W}$ as:

$$\mathbf{I} = \mathbf{R} \odot \mathbf{L}, \tag{2}$$

where $\odot$ denotes the element-wise multiplication. However, this corruption-free assumption is consistent with the real under-exposed scenes, where corruptions are inevitably introduced by the high-ISO and long-exposure imaging settings, as well as the light-up process. To model the corruptions, they introduce perturbation terms for $\mathbf{R}$ and $\mathbf{L}$ and reformulate Eq. (2) as:

$$\begin{aligned}\mathbf{I} &= (\mathbf{R} + \hat{\mathbf{R}}) \odot (\mathbf{L} + \hat{\mathbf{L}}) \\ &= \mathbf{R} \odot \mathbf{L} + \mathbf{R} \odot \hat{\mathbf{L}} + \hat{\mathbf{R}} \odot (\mathbf{L} + \hat{\mathbf{L}}).\end{aligned} \tag{3}$$

$\hat{\mathbf{R}} \in \mathbb{R}^{H\times W\times 3}$ and $\hat{\mathbf{L}} \in \mathbb{R}^{H\times W}$ are the perturbations. To light up $\mathbf{I}$, they multiply two sides of Eq. (3) by a light-up map $\bar{\mathbf{L}}$ such that $\bar{\mathbf{L}} \odot \mathbf{L} = \mathbf{1}$ as:

$$\mathbf{I} \odot \bar{\mathbf{L}} = \mathbf{R} + \mathbf{R} \odot (\hat{\mathbf{L}} \odot \bar{\mathbf{L}}) + (\hat{\mathbf{R}} \odot (\mathbf{L} + \hat{\mathbf{L}})) \odot \bar{\mathbf{L}}, \tag{4}$$

They then simplify Eq. (4) as

$$\mathbf{I}_{lu} = \mathbf{I} \odot \bar{\mathbf{L}} = \mathbf{R} + \mathbf{C}, \tag{5}$$

where $\mathbf{I}_{lu} \in \mathbb{R}^{H\times W\times 3}$ denotes the lit-up image and $\mathbf{C} \in \mathbb{R}^{H\times W\times 3}$ indicates the overall corruption term. Subsequently, they formulate their ORF as:

$$(\mathbf{I}_{lu}, \mathbf{F}_{lu}) = \mathcal{E}(\mathbf{I}, \mathbf{L}_p), \quad \mathbf{I}_{en} = \mathcal{R}(\mathbf{I}_{lu}, \mathbf{F}_{lu}), \tag{6}$$

where $\mathcal{E}$ denotes the illumination estimator and $\mathcal{R}$ represents the corruption restorer. $\mathcal{E}$ takes $\mathbf{I}$ and its illumination prior map $\mathbf{L}_p \in \mathbb{R}^{H\times W}$ as inputs. $\mathbf{L}_p$ = mean$_c(\mathbf{I})$ where mean$_c$ calculates the average pixel values across channels. $\mathcal{E}$ outputs the lit-up image $\mathbf{I}_{lu}$ and light-up feature $\mathbf{F}_{lu} \in \mathbb{R}^{H\times W\times C}$. Then $\mathbf{I}_{lu}$ and $\mathbf{F}_{lu}$ are fed into $\mathcal{R}$ to restore the corruptions and produce the enhanced image $\mathbf{I}_{en} \in \mathbb{R}^{H\times W\times 3}$.

Illumination Estimator. The architecture of $\mathcal{E}$ is shown in Fig. 2 (a) (i). $\mathcal{E}$ firstly uses a $conv$1×1 (convolution with kernel size = 1) to fuse the concatenation of $\mathbf{I}$ and $\mathbf{L}_p$. The well-exposed regions can provide semantic contextual information for under-exposed regions. Thus, a depth-wise separable $conv$9×9 is adopted to model the interactions of regions with different lighting conditions to generate the light-up feature $\mathbf{F}_{lu}$. Then $\mathcal{E}$ uses a $conv$1×1 to aggregate $\mathbf{F}_{lu}$ to produce the light-up map $\bar{\mathbf{L}} \in \mathbb{R}^{H\times W\times 3}$, which is used to light up $\mathbf{I}$ in Eq. (4).

Illumination-Guided Transformer. As illustrated in Fig. 2 (a) (ii), IGT adopts a three-scale U-shaped architecture [10, 13–16]. The input of IGT is the lit-up image $\mathbf{I}_{lu}$. In the downsampling branch, $\mathbf{I}_{lu}$ undergoes a $conv$3×3, an IGAB, a strided $conv$4×4, two IGABs, and a strided $conv$4×4 to generate hierarchical features $\mathbf{F}_i \in \mathbb{R}^{\frac{H}{2^i}\times\frac{W}{2^i}\times 2^i C}$ where i = 0, 1, 2. Then $\mathbf{F}_2$ passes through two IGABs. Subsequently, a symmetrical structure is designed as the upsampling branch. Skip connections are used to alleviate the information loss caused by the downsampling branch. The upsampling branch outputs a residual image $\mathbf{I}_{re} \in \mathbb{R}^{H\times W\times 3}$. Then the enhanced image $\mathbf{I}_{en}$ is derived by the sum of $\mathbf{I}_{lu}$ and $\mathbf{I}_{re}$, *i.e.*, $\mathbf{I}_{en}$ = $\mathbf{I}_{lu}$ + $\mathbf{I}_{re}$.

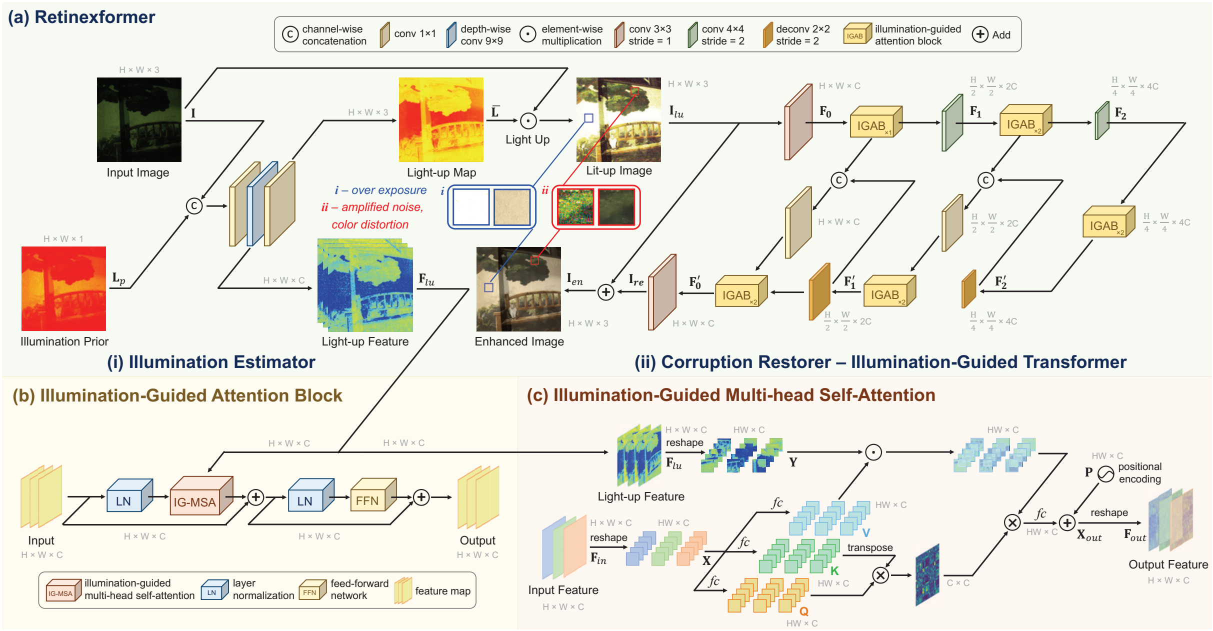

Figure 2. The overview of Retinexformer [8]. (a) Retinexformer adopts the proposed ORF that consists of an illumination estimator (i) and a corruption restorer (ii) IGT. (b) The basic unit of IGT is IGAB, which is composed of two layer normalization (LN), an IG-MSA and a feed-forward network (FFN). (c) IG-MSA uses the illumination representations captured by ORF to direct the computation of self-attention.

IG-MSA. As illustrated in Fig. 2 (c), the light-up feature $\mathbf{F}_{lu} \in \mathbb{R}^{H\times W\times C}$ estimated by $\mathcal{E}$ is fed into each IG-MSA of IGT. Firstly, the input feature is reshaped into tokens $\mathbf{X} \in \mathbb{R}^{HW\times C}$ and split into k heads:

$$\mathbf{X} = [\mathbf{X}_1,\ \mathbf{X}_2,\ \cdots,\ \mathbf{X}_k], \tag{7}$$

where $\mathbf{X}_i \in \mathbb{R}^{HW\times d_k}$, $d_k = \frac{C}{k}$, and $i = 1, 2, \cdots, k$. Then $\mathbf{X}_i$ is linearly projected into *query* $\mathbf{Q}_i$, *key* $\mathbf{K}_i$, and *value* $\mathbf{V}_i \in \mathbb{R}^{HW\times d_k}$ as:

$$\mathbf{Q}_i = \mathbf{X}_i\mathbf{W}^{\mathrm{T}}_{\mathbf{Q}_i},\ \ \mathbf{K}_i = \mathbf{X}_i\mathbf{W}^{\mathrm{T}}_{\mathbf{K}_i},\ \ \mathbf{V}_i = \mathbf{X}_i\mathbf{W}^{\mathrm{T}}_{\mathbf{V}_i}, \tag{8}$$

where $\mathbf{W}_{\mathbf{Q}_i}$, $\mathbf{W}_{\mathbf{K}_i}$, and $\mathbf{W}_{\mathbf{V}_i} \in \mathbb{R}^{d_k\times d_k}$ are learnable parameters and T denotes the matrix transpose. Subsequently, they use the light-up feature $\mathbf{F}_{lu}$ encoding illumination information and interactions of regions with different lighting conditions to direct the computation of self-attention. They reshape $\mathbf{F}_{lu}$ into $\mathbf{Y} \in \mathbb{R}^{HW\times C}$ and split it into k heads:

$$\mathbf{Y} = [\mathbf{Y}_1,\ \mathbf{Y}_2,\ \cdots,\ \mathbf{Y}_k], \tag{9}$$

where $\mathbf{Y}_i \in \mathbb{R}^{HW\times d_k}$, $i = 1, 2, \cdots, k$. Then self-attention is formulated as:

$$\text{Attention}(\mathbf{Q}_i, \mathbf{K}_i, \mathbf{V}_i, \mathbf{Y}_i) = (\mathbf{Y}_i \odot \mathbf{V}_i)\text{softmax}(\frac{\mathbf{K}^{\mathrm{T}}_i\mathbf{Q}_i}{\alpha_i}), \tag{10}$$

where $\alpha_i \in \mathbb{R}^1$ is learnable parameter. Subsequently, k heads are concatenated to pass through an fc layer and plus a learnable positional encoding $\mathbf{P} \in \mathbb{R}^{HW\times C}$ to produce the output tokens $\mathbf{X}_{out} \in \mathbb{R}^{HW\times C}$. Finally, they reshape $\mathbf{X}_{out}$ to derive output feature $\mathbf{F}_{out} \in \mathbb{R}^{H\times W\times C}$.

Besides Retinexformer [8], the team also adopt their winning solution MST [11, 12] of NTIRE 2022 Spectral Recovery Challenge [2] as an auxiliary method for ensemble. The code is released at https://github.com/caiyuanhao1998/MST and https://github.com/caiyuanhao1998/MST-plus-plus.

Implementation: Retinexformer is implemented by PyTorch. The model is trained with the Adam [41] optimizer (β_1 = 0.9 and β_2 = 0.999) for 2.5×10^5 iterations. The learning rate is initially set to 2×10^{-4} and then steadily decreased to 1×10^{-6} by the cosine annealing scheme [52] during the training process. Patches at the size of 2000×2000 are randomly cropped from the low-/normal-light image pairs as training samples. The batch size is 8. The training data is augmented with random rotation and flipping. The training objective is to minimize the mean absolute error (MAE) between the enhanced image and ground-truth image. The team use the mixed-precision training strategy (also the amp in Pytorch).

In the testing phase, images with the size of 2000×3000 are directly fed into the network. Images with the size of 4000×6000 are firstly split into two 4000×3000 images to undergo the model and then merged to obtain the enhanced images. Self-ensemble and multi-model ensemble strategies are used for final testing.

4.3. DH-AISP

Description: DWT-FFC [83] is employed as the backbone in our proposed method for low-light image enhancement. Dark light usually results in degraded image quality, low contrast, color shift, and structural distortion. We have observed that many deep learning-based models show superior performance in dark light enhancement, but they are generally not up to the challenge of lower light. There are two main factors contributing to this. First, due to the uneven distribution of image brightness, it is very challenging to recover structure and chromaticity features with highfdelity, especially in areas of extremely low brightness. Secondly, the existing small-scale data sets for dark light enhancement are not sufcient to support reliable learning of feature mapping based on convolutional neural network (CNN) models. To address these two challenges, we employ a novel two-branch network utilizing two-dimensional discrete Walsh transform (DWT), fast Fourier Convolution (FFC) residual blocks, and a pre-trained ConvNeXt model. Specifcally, in the DWT-FFC frequency branch, our model utilizes DWT to capture more high-frequency features. In addition, by utilizing the large receptive feld provided by FFC residuals, our model is able to efciently explore global context information and generate images with better perceptual quality. In the prior knowledge branch, we use the pre-trained ImageNet ConvNeXt instead of Res2Net. This allows our model to learn more complementary information and gain greater generalization ability. The feasibility and effectiveness of the proposed method are proved by extensive experiments.

Implementation: The training dataset is based solely on data provided by the competition organizers. The training images are generated by random clipping, and the training GPU is RTX 4080. A training session takes about 48 hours on a single GPU. The optimizer uses Adam. The initial learning rate is 0.0001, halved every 500 epochs.Training in python based on pytorch platform.

4.4. NWPU-DiffLight

Description: As shown in Fig. 3, we proposed a dual-branch pipeline called DiffLight. Besides, we proposed a method, Progressive Patch Fusion (PPF) for high-resolution image restoration. Given a low-light image as input, it will be fed into the two branches separately. In the DE branch (Fig. 3 (a)), the low-quality image is processed sequentially by DiffIR [5] and LEDNet [65] to get the image enhanced by DE branch, $Output_{DE}$:

$$\mathbf{Output}_{DE} = \text{LEDNet}(\text{DIffBackward}(\mathbf{Input})), \quad (11)$$

where DiffBackward$(\cdot)$ represents the the Backward Process of DiffIR (which is for inference). The enhanced image, $Output_{DE}$, has fairly low noise, minimal color deviation, as well as highly-increased brightness, but there is an excessive loss of details.

In the DP branch (Fig. 3 (b)), the newly proposed method for high-resolution image restoration, PPF, is used. To better recover the details from high-resolution images, the image is divided into n small low-quality (LQ) overlapping patches in the Segmentation process, the patch size is adapted to the input size for training. Each patch is individually processed through the Restormer to obtain n high-quality (HQ) overlapping patches. To get $Output_{DP}$, the image enhanced by DP-branch, PPF is applied on these enhanced patches:

$$\mathbf{Output}_{DP} = \text{PPF}(\text{Restormer}(\text{Segmentation}(\mathbf{Input}))). \quad (12)$$

The block artifacts produced by the traditional fusion method is removed by PPF, providing good visual quality and rich details. Finally, $Output_{DE}$ and $Output_{DP}$ are multiplied by weights w_1 and w_2 respectively, and summed to form the final output image after weighted averaging:

$$\mathbf{Output} = w_1\mathbf{Output}_{DE} + w_2\mathbf{Output}_{DP}. \quad (13)$$

Progressive Patch Fusion. For high-resolution images, we utilize the Progressive Patch Fusion (PPF) method during testing. This approach incorporates progressive weight management at the to effectively mitigate edge and substantially improve visual fidelity. PPF is performed by these steps as follows:

1. Image Segmentation: The input image I is segmented into patches of size p. These patches slide across the image with a stride (s) of stride to determine their locations.
2. Model Inference: The model is used to sequentially infer each patch, resulting in inferred patches.
3. Weight Calculation: Four weight tensors, $weight_{1,2,3,4}$ are computed for blending overlapping regions. The weights for overlapping regions linearly range from 1 to 0. $weight_{1,2}$ are used for blending overlaps between patches, while $weight_{3,4}$ are used for merging overlaps between rows.
4. Image Reconstruction: Initialize an empty restore image and $patch_{row}$ row image, which will be used to store the reconstructed image and the current row being processed.
5. Fusion Process:
   - For each h_i (row index) and w_i (column index), extract the corresponding patch from the patches tensor. If it is the first patch of the row (w_i equals 0), add it directly to the $patch_{row}$.
   - For subsequent patches, use $weight_{1,2}$ to blend the overlapping regions between the two patches.
   - Add the processed $patch_{row}$ to the restored image I'.
   - If it is not the first row ($h_i \neq 0$), blending between rows using $weight_{3,4}$ is required.

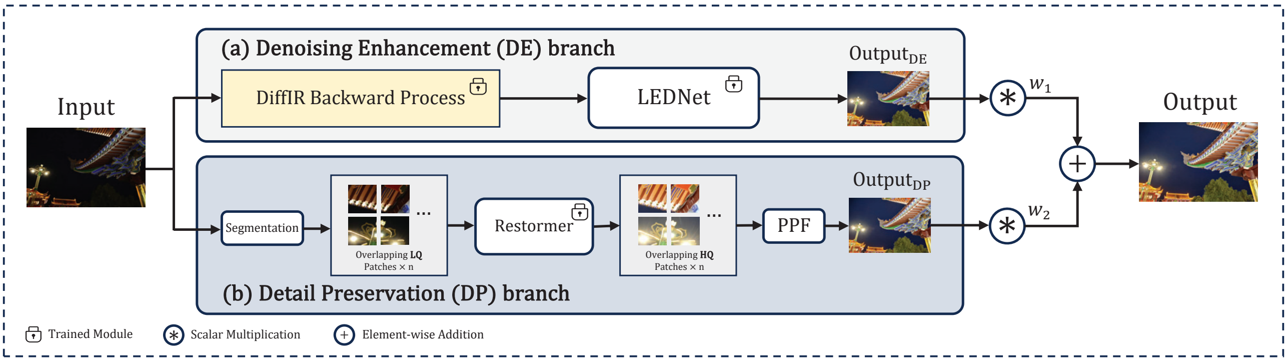

Figure 3. DiffLight pipeline. DiffLight is composed of two branches: (a) Denoising Enhancement (DE) branch and (b) Detail Preservation (DP) branch.

6. Output: the aforementioned steps, restore tensor contains the the restored image I'.

Implementation: For the Denoising Enhancement (DE) branch, we train DiffIR [5] and LEDNet [65] separately. In training the diffusion model, total timesteps T are set to 4, and β_t linearly increase from $\beta_1 = 0.9$ to $\beta_T = 0.99$. We train the two stage of DiffIR [5] only using $\mathcal{L}_1$ loss. We train DiffIR$_{S1}$ for 300K iterations with the initial learning rate 2×10^{-4} gradually reduced with the cosine annealing. And For DiffIR$_{S2}$, we train 300K iterations with initial learning rate 2×10^{-4} and gamma 0.5 with the MultiStepLR scheduler. For both training stage, we progressively increase patch size and decrease batch size. Specifically, during iterative training, the patch size and batch size pair are set to respectively train for $(92K)$, $(80K)$, $(38K)$, $(90K)$ iterations under the configurations of $(192, 8)$, $(256, 4)$, $(320, 2)$, $(400, 1)$.

LEDNet [65] model is trained on the inference results on Train set produced by DiffIR, and the Ground Truth remains unchanged. We train LEDNet using Adam [41] optimizer with $\beta_1 = 0.9$, $\beta_2 = 0.99$ for a total of 300k iterations. The initial learning rate is set to 1×10^{-4} and updated with cosine annealing strategy [52]. Similar to DiffIR, we still adopt a progressive training approach, the patch size and batch size pair are set to train for $(90K)$, $(70K)$, $(70K)$, $(70K)$ iterations respectively under the configurations of $(256, 8)$, $(512, 4)$, $(1024, 1)$, $(1320, 1)$.

We implement our the Detail-Preservation (DP) branch by PyTorch. The model is trained with the Adam [41] optimizer (β_1 = 0.9 and β_2 = 0.999) for at least 300 epochs by using a single NIVIDA 3090 GPU. The learning rate is initially set to 1×10^{-4} and then steadily decreased to 1×10^{-7} by the cosine annealing scheme [52] during the training process. We randomly crop the image to 256×256 for patch size and set batch size to 8. When testing, we use our proposed Progressive Patch Fusion (PPF) method that addresses edge artifacts and yields favorable visual perceptual results with high resolution images.

4.5. GiantPandaCV

Description: Existing restoration backbones are usually limited due to the inherent local reductive bias or quadratic computational complexity in Ultra-High-Defnition (UHD) image restoration tasks. Recently, Selective Structured State Space Model, *e.g.* , Mamba [50], has shown great potential for long-range dependencies modeling with linear complexity. Therefore, we introduce the Selective Structured State Space Model [33] into the low light image enhancement task and propose an efficient model for UHD images, named UHDMamba. Specifically, our UHDMamba uses the Residual State Space Block as the core component, which employs convolution and channel attention to enhance the capabilities of the vanilla Mamba. To efficiently infer UHD images, we used PixelUnshuffle to downsample the UHD images and then input them into the network for enhancement. Finally, we used PixelShuffle upsampling to reconstruct the final image.

The main architecture of the UHDMamba is shown in Fig. 4, which consists of three components: Shallow feature extraction, Deep feature enhancement, and Upsampling reconstruction. Given a low-quality (LQ) input image $I_{LQ} \in \mathcal{R}^{H \times W \times 3}$, we first employ a 3×3 convolution layer from the shallow feature extraction to generate the shallow feature $F_s \in \mathcal{R}^{H \times W \times \frac{C}{S}}$, where H and W represent the height and width of the input image, C is the number of channels, and S is the downsample scale factor. Subsequently, the shallow feature F_s undergoes downsample operation and the deep feature enhancement stage to acquire the deep feature $F_d^l \in \mathcal{R}^{\frac{H}{S} \times \frac{W}{S} \times SC}$ at the $l-$th layer, $l \in 1, 2, ..., L$. This stage is stacked by multiple Residual State-Space Blocks (RSSBs). Finally, we use the element-wise sum to obtain the input of the high-quality reconstruction stage $F_R = F_L + F_s$, which is used to Upsample reconstruct the high-quality (HQ) output image I_{HQ}.

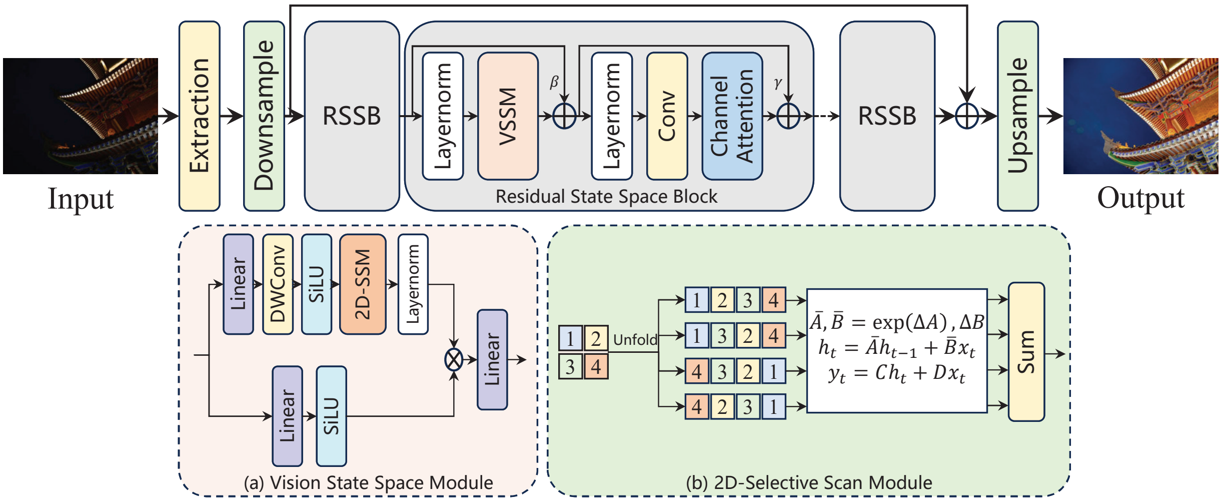

Figure 4. An overview of our UHDMamba for UHD Low Light Enhancement.

Implementation: The proposed method conducts experiments in PyTorch on two NVIDIA GeForce RTX 3090 GPUs. To optimize the network, the model employs the Adam [41] optimizer with a learning rate 2×10^{-4}. We randomly crop the full-resolution image to a resolution of 512×512 as the input and perform 200k iterations of training with a batch size of 4. To augment the training data, random horizontal and vertical flips are applied to the input images. The number of RSSB and feature channels is set to 8 and 48, respectively. DownSampler and UpSampler are both composed of a sub-pixel convolutional layer.

In order to maximize the potential performance of our model, the method adopts the Test Time Augmentation strategy (TTA). During the test time, it used $90°, 180°, 270°$ rotation, horizontal flip, and vertical flip to generate six augmented inputs $\{I_{n,i}^{input} = T_i(I_n^{input})\}$ from input left and right images I_n^{input}. With those augmented input images and the original input image, we generate corresponding clear images $\{I_{n,1}^{output}, \cdots, I_{n,6}^{output}\}$ using the networks. We then apply an inverse transform to those output images to get the original geometry $\tilde{I}_{n,i}^{output} = T_i^{-1}(I_{n,i}^{output})$. Finally, we average the transformed outputs altogether to make the TTA result as follows. $I_n^{output} = \frac{1}{6}\sum_{i=1}^{6} \tilde{I}_{n,i}^{output}$.

4.6. LVGroup_HFUT

Description: Low light enhancement refers to a process or set of techniques in computer vision aimed at improving the visual quality of images by adjusting their lighting conditions. This process can involve increasing the brightness and contrast, correcting underexposed or overexposed areas, and enhancing details in shadows and highlights. The goal is to produce images that more accurately reflect the scene as perceived by the human eye, even under less-than-ideal lighting conditions. However, complex models are difficult to reason about on the GPU, limited by the larger image resolution. Therefore, NAFNet [18] is chosed as baseline and further lighten NAFNet based on it to get a brand new structure. Specifically, the number of channels is kept constant at the early stage of the encoding phase and at the end of the decoding phase, while the up- and down-sampling operations are performed, as shown in Fig. 5.

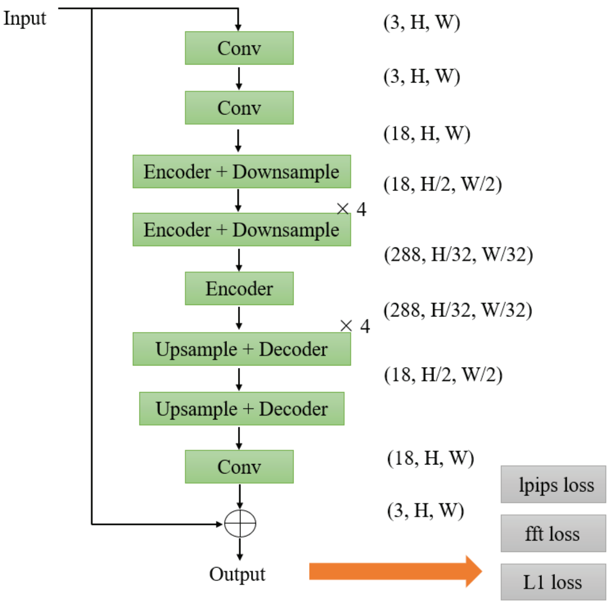

Figure 5. The network architecture of team LVGroup_HFUT.

More specifically, the input image is initially subjected to pixel alignment and convolution operations, during which the number of channels is expanded from 3 to 8. Subsequently, the image passes through an encoder and a downsampling module, resulting in an increase in channel count to 288, while its dimensionality is reduced to one-thirty-second of its original size. Following this, a decoder accompanied by an upsampling module is applied, which adjusts the channel count to 18 and restores the dimensions to their original size. The final output is then obtained through a convolutional layer. During the training process, the model is constrained using a combination of lpips loss, fft loss, and L1 loss to optimize performance and ensure fidelity to the input image.

Implementation: The proposed architecture is based on PyTorch 2.2.1 and an NVIDIA 4090 with 24G memory. 2000 epochs are set for training with batch size 2, using AdamW with $\beta_1 = 0.9$ and $\beta_2 = 0.999$ for optimization. The initial learning rate was set to 0.001, and cosine annealing was used for learning rate adjustment. The randomly crop the image to 768×768 is first performed and then horizontal flip with probability 0.5 is performed for data augment. The input image is fed into the network, and it is constrained using three loss functions: lpips loss with weight 0.5, fft loss with weight 0.1, and L_1 loss with weight 1.

The testing process begins by combining a total of 10 equally-spaced checkpoints obtained in training phase. Specifically, the input image with original resolution sequentially passes through these 10 checkpoints, resulting in 10 outputs. Finally, the model ensemble strategy is applied to process these 10 outputs, yielding the ultimate output. Besides, since the test set contains images with too large resolution (4000×6000), A100 (40G memory) is used for inference to avoid the 'cuda out of memory' error.

4.7. Try1try8

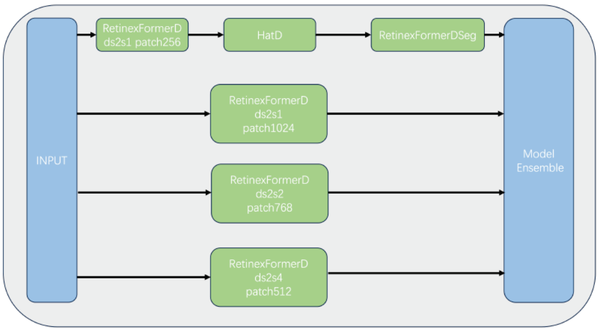
INPUT
RetinexFormerD ds2s1 patch256
HatD
RetinexFormerDSeg
RetinexFormerD ds2s1 patch1024
RetinexFormerD ds2s2 patch768
RetinexFormerD ds2s4 patch512
Model Ensemble

Figure 6. The network architecture of team Try1try8.

Description: Due to the large resolution of the inference images, the authors added a downsampling operation to the RetinexFormer, renaming it to RetinexFormerD. The authors employed a RetinexFormerD model architecture with varying training patch sizes, and cascaded it with a denoising model (HatD) and a fine-tuning model(RetinexFormerDseg). Finally, the authors performed a model ensemble of all the model results. The model is shown in Fig. 6.

Implementation: *path1:* Initially, the authors applied downsampling to the RetinexFormer to create RetinexFormerD (due to the large size of the inference images), followed by the use of the HATD model (which incorporates the HAT model with downsampling) to denoise the inference results of RetinexFormerD. Ultimately, RetinexFormerSeg (which integrates image segmentation results into the model) was utilized to fine-tune the final results. *path2:* The authors trained RetinexFormerD with various patch sizes and stages, resulting in three Retinex-FormerD models: RetinexFormerD ds2s1 with a patch size of 1024, RetinexFormerD ds2s2 with a patch size of 768, and RetinexFormerD ds2s4 with a patch size of 512. Finally, the authors averaged the results obtained from path1 and path2. The model is trained with Adam optimizer, 2e-4 as learning rate, and on V100

4.8. Pixel_warrior

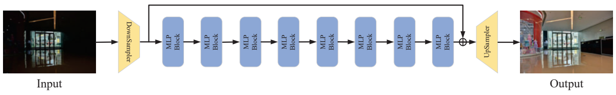

Figure 7. The network architecture of team Pixel_warrior.

Description: The team proposes an efficient vision MLP-based architecture for low-light enhancement (see Fig. 7). Our MLP block contains dimension transformation operations (see Fig. 8). Specifically, we first normalize the input features, and then perform multi-stage dimension transformations to rotate the spatial perspective of tensors across 3 dimensions of H, W and C. Here, the 3D feature map undergoes recursive encoding from (C, H, W) to (H, W, C) and then to (W, C, H), enabling the capture of global spatial information through multi-view dimensions. Finally, we adjust the feature map to the original resolution, and interact with the input features to activate useful features.

Implementation: We conduct network training on four NVIDIA Tesla V100 GPUs with 32GB memory. In total, we perform 500 epochs of training. During the training, we adopt the Adam optimizer with a learning rate of 2×10^{-4}. The patch size is set to be 2000×2000 pixels and the batch size is set to be 4. To augment the training data, we apply random horizontal and vertical flips.

4.9. HuiT

Description: The team introduced LLformer [69] to address this issue. As shown in Fig. 9, given a low-light image, LLformer first extracts shallow features f_0, which are then fed into three sequential Transformer blocks to extract deep features. Specifically, the intermediate features

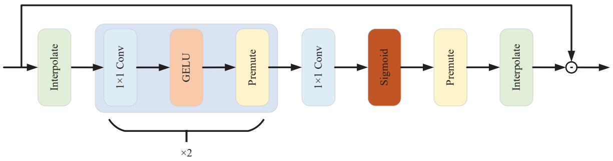

Figure 8. The network architecture of the MLP block.

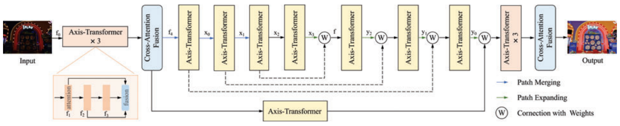

Figure 9. Illustration of the propsed LLformer.(Re-produced from LLformer [69])

output from the Transformer blocks are denoted as f_1, f_2, f_3. These features are aggregated and transformed into enhanced image features f_4 using the proposed cross-layer attention fusion block. Subsequently, deep feature extraction is performed on f_4 using four stages in the encoder. Specifically, each stage includes Patch Merging and Axis-Transformer blocks. Then, the low-resolution latent features are gradually restored to a high-resolution representation using the decoder, which consists of three stages and takes x_3 as input. Each stage consists of Patch Expanding and Axis-Transformer blocks. To reduce information loss at the encoding end and achieve better feature restoration at the decoding end, weighted skip connections with 1×1 convolutions are used for feature fusion in both the encoding and decoding ends. Thirdly, after decoding, the deep features f are sequentially processed through three Axis-Transformer blocks and a cross-layer attention fusion block to generate enhanced features for image reconstruction. Finally, the enhanced image is produced. The Axis-Transformer block, as shown in Fig. 10, performs self-attention mechanism along the height and width axes of the features in the cross-channel dimension to capture non-local self-similarity and long-range correlations with lower computational complexity. The Cross-Attention Fusion block, as shown in Fig. 11, learns attention weights between different layer features and adaptively fuses features with the learned weights to improve feature representation.

Implementation: The code is implemented based on the Pytorch framework, We trained the model in 300 epochs on two NVIDIA 4090 GPU with batchsize of 24. The model are optimized by the Adam with β_1 = 0.9 and β_2 = 0.999 with weight decay 1e-8 by default. The initial learning rate was set to 2e-4, and true cosine annealing was chosen as the learning scheme. The loss function is defined as:

$$\pounds_{total} = \pounds_{pix} + \lambda \pounds_{ssim}, \tag{14}$$

where $\pounds_{pix}$ represents the L1 Loss, and $\pounds_{ssim}$ signifies the SSIM Loss. The parameter λ denotes the loss weight used to balance the influence between the two terms. In our experiments λ is set to 1.0.

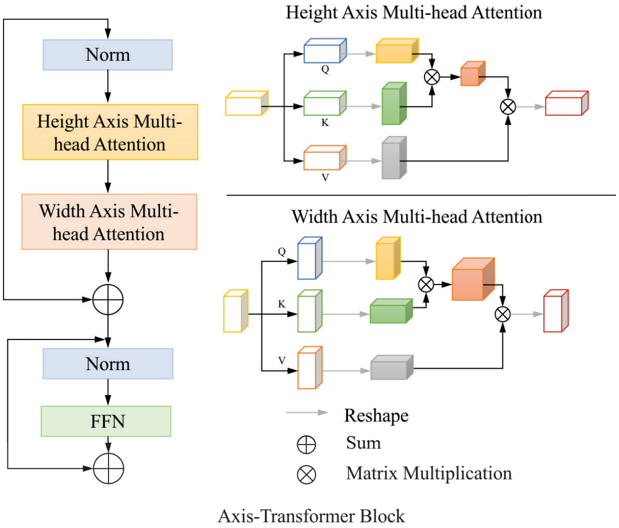
Norm
Height Axis Multi-head Attention
Width Axis Multi-head Attention
Norm
FFN
Height Axis Multi-head Attention
Q
K
V
Width Axis Multi-head Attention
Q
K
V
Reshape
Sum
Matrix Multiplication
Axis-Transformer Block

Figure 10. Illustration of the proposed Axis-Transformer Block.

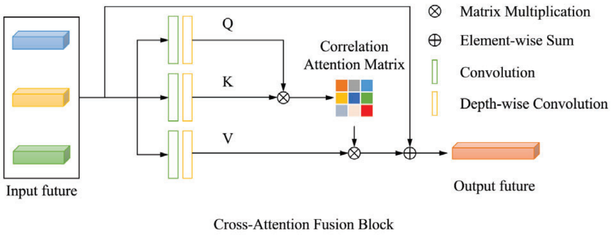

Figure 11. Illustration of the proposed Cross-Attention Fusion Block.

To save computational resources, high-definition images need to be chunked, however, the size of the patches has a great impact on the results. Experiments have shown that the best results will be achieved by segmenting the original image of size 2000 × 2996 into multiple patches of size 500 × 748, and by segmenting the original image of size 4000 × 6000 into patches of size 800 × 1200. We randomly cropped 128 × 128 smaller patches from the processed images during the network training process. Following the data augmentation techniques outlined in the LLFormer [69] methodology, we applied random horizontal and vertical flips to these patches.

4.10. X-LIME

Description: Our method consists of two modules, which are the curve estimation network for lightness adaption and the denoising network for denoising. Specifically, we adopt Zero-DCE [34] as a lightness adaption network and

NAFNet [19] as a denoising network. For better lightness adaption performance, we adjust the relevant loss function. Specifically, we add MSELoss to the original Zero-DCE [35] loss and train for 10 epochs on the provided dataset. In the training phase, we use Zero-DCE pre-trained weights provided in the official Github repository and fine-tune the provided dataset for the first stage. For the second stage, we used NAFNet [19] pre-trained on the SIDD dataset and fine-tuned the output of the lightness module. In the testing phase, we first use the lightness adaption module to adapt the lightness, thus increasing the contrast in the image. Then we feed the output of the lightness module into the denoising module to further mitigate the noise.

Implementation: Our proposed method is implemented in Python with the help of the PyTorch framework. The models used in the two stages are optimized with Adam. In the first stage, the learning rate is set to 1e-4 and in the second stage, the learning rate is set to 5e-5, respectively. In the first stage, we adapt the RTX4090 GPU while the A100 80G is used in the second stage. The convergence speed of the first stage is rather fast, so we only train 10 epochs on the training set with the full image as input, resulting in a 30-minute training. For the second stage, we train the NAFNet [19] with a progressively enlarged patch strategy. The first 30000 iterations are trained with 512×512 patches, then we enlarge the training patch to 1024×1024 for 25000 iterations. Finally, we use 1920×1920 patches for 10000 iterations. During testing, we use TLC [21] to further boost the performance of our patch-based method. The base size of TLC is set to (1920, 2980).

4.11. Image Lab

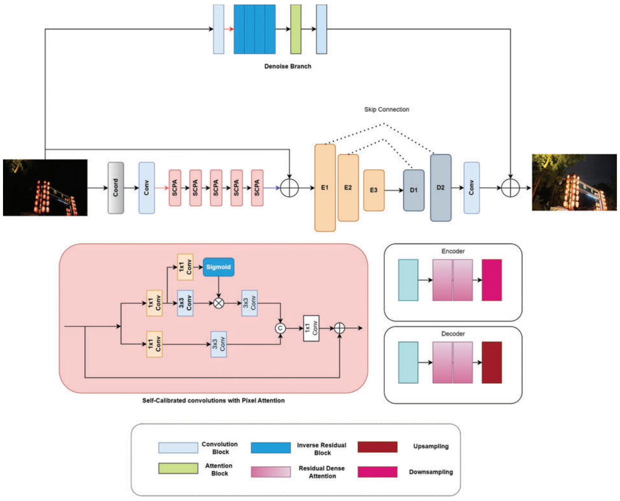

Figure 12. Architecture Diagram of ImageLab Team's Demosaicing Model

Description: We propose a novel image denoising and enhancement architecture, leveraging the power of Coordinate Convolution (CoordConv) [46] layers and Self-Calibrated Convolution with pixel attention (SCPA) blocks [61, 85], as shown in Fig. 12. The architecture is designed to suppress noise while effectively preserving important image details.

The input image is first passed through a CoordConv layer to add channels containing hard-coded coordinates, enriching the representation with spatial information. This augmented representation is then downsampled and fed into five consecutive SCPA layers with a Pixel Attention Block. SCPA layers enhance the model's capture of intricate spatial patterns and features. The output from the SCPA layers is upsampled and added back to the input image. This combined representation is passed through a Modified U-Net architecture with Residual Dense Channel Attention (RDCA) blocks [60]. The U-Net consists of three encoder blocks and two decoder blocks. Each encoder block contains two RDCA blocks followed by downsampling, while each decoder block contains two RDCA blocks followed by upsampling. This design facilitates the extraction and refinement of features at multiple scales. Simultaneously, the input image is fed into a sophisticated denoising block [22] to produce a three-channel denoised image. The denoising block comprises four inverse convolutional layers followed by an attention mechanism. This mechanism effectively suppresses noise while preserving important image details, enhancing the overall quality of the denoised image. The outputs of the RDCA-UNet and the denoising block are added to the input image, resulting in a final enhanced image combining the denoising block's denoised features with the refined features from the RDCA-UNet.

Implementation: The proposed network was trained using the NVIDIA Tesla P100 with 16GB RAM and the TensorFlow Keras platform. 400x400x3 patches were randomly extracted from the images. The training dataset consisted of 4281 patches, and 755 patches were used for validation. Augmentation techniques were applied during training. The model was optimized using the Adam optimizer with a learning rate schedule that decreased from 0.001 to 0.00001 over 250 epochs. The model comprises 0.437556 million parameters. The training objective included a combination of $\mathcal{L}_1$, $\mathcal{L}_{SSIM}$, and $\mathcal{L}_{Grad}$ loss, *i.e.* ,

$$\mathcal{L} = 0.1 * \mathcal{L}_{SSIM} + \mathcal{L}_1 + \mathcal{L}_{Grad}. \tag{15}$$

4.12. dgzzqteam

Description: The author claimed that the solution is based on the published OGF, while not providing the specific citation. The authors changed the loss function and fine-tuned the model so that it could perform better in the competition.

Implementation: The authors implement the OGF by PyTorch. The model is trained with the Adam optimizers (β_1 = 0.9 and β_2 = 0.999) for 2.5 × 105 iterations. The learning rate is initially set to $2e$-4 and then steadily decreased

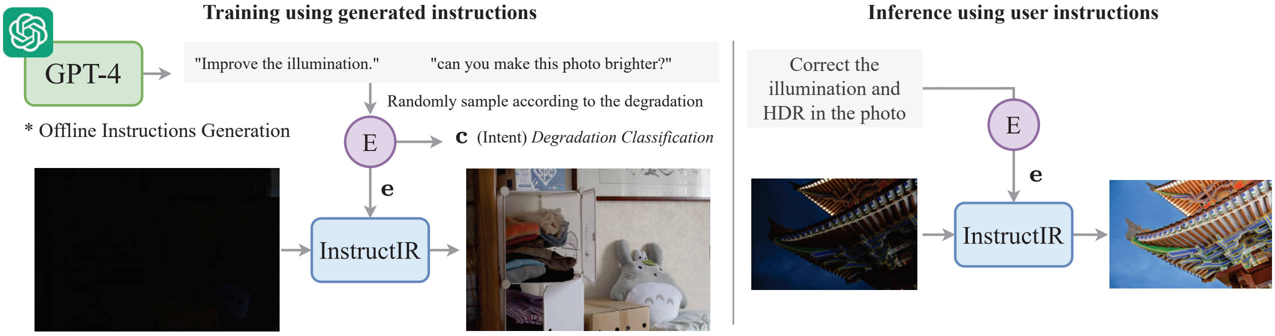
Training using generated instructions
GPT-4
"Improve the illumination."
"can you make this photo brighter?"
Randomly sample according to the degradation
* Offline Instructions Generation
E
c (Intent) Degradation Classification
e
InstructIR
Inference using user instructions
Correct the illumination and HDR in the photo
E
e
InstructIR

Figure 13. **InstructIR** [23] takes as input an image and a human-written instruction for how to improve that image. The multi-task model performs text-guided low-light image enhancement.

to 1e-6 by the cosine annealing scheme during the training process. Patches at the size of 128 × 128 are randomly cropped from the low-/normallight image pairs as training samples. The batch size is 8. The training objective is to minimize the mean absolute error (MAE) between the lit-up image and the enhanced image. The training and validation sets are split in proportion to 209:21.

4.13. Cidaut AI

Description: We use **InstructIR** [23] for real-world low-light enhancement. InstructIR [23] takes as input an image and a human-written instruction for how to improve that image. The neural model performs all-in-one image restoration. InstructIR [23] achieves state-of-the-art results on several restoration tasks including image denoising, deraining, deblurring, dehazing, and (low-light) image enhancement. The approach is illustrated in Fig. 13.

The model achieves 23.07 dB, 0.8075 SSIM and 0.156 LPIPS in the NTIRE 2024 Low-light Enhancement Challenge, *representing a baseline solution for multi-task restoration using text-guidance.*

Implementation: The model can process full-resolution images in a regular GPU without tiling strategies. We fine-tune the model using the challenge dataset besides LOL [71]. We use the instructions *"correct the low illumination in this image"* for all the test images.

Efficient Baseline Methods: The team also studies efficient methods that can process full-resolution images in real-time at several FPS: RetinexNet [71], SCI [55] and Zero-DCE [34]. All these methods can process 4000 × 6000 directly on regular GPUs such as Nvidia 3090Ti. However, these methods did not improve over InstructIR [23].

Datasets: To enhance our results and generalize better, we included other training datasets: LOL-v2 (real and synthetic) and the MIT5K dataset. We also apply random crop, flip and rotation augmentations.

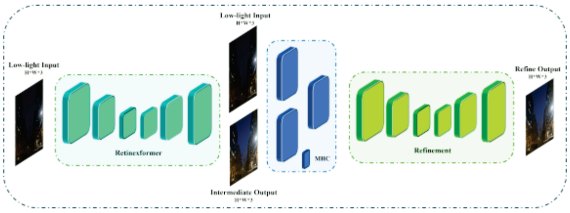

Figure 14. Overall framework the Team OptDev's DFormer

4.14. OptDev

Description: The authors developed a novel transformer-based deep network DoubleFormer (DFormer) to learn low-light to highlight mapping, as shown in Fig. 14. The architecture comprises two separate encoder-decoder blocks (EDB) and a multi-head correlation block (MHCB) to produce plausible images. The authors leverage illumination mapping from the well-known Retinex theory to accelerate our reconstruction performance. Also, the authors incorporated the state-of-the-art low-light enhancement method, Retinexformer in the overall architecture's first half. Regrettably, Retinexformer failed to generate plausible images in many tricky scenes while illustrating visible noise and color desaturation in complex regions. To address this limitation, the authors proposed to utilize an MHCB, followed by another EDB in our architecture. We leverage the correlated features with intermediate output in the second EDB to perceive better denoising results. In addition to that, the authors utilized a perceptual loss, including luminance-chrominance guidance, to address the color inconsistency.

Implementation: The proposed solution is implemented with the PyTorch framework. The networks were optimized with a Adam optimizer, where the hyperparameters were tuned as β_1 = 0.9, β_2 = 0.99, and learning rate = 5e-4. We trained our model with non-overlapping image patches with a constant batch size of 12, which takes around 36 hours to complete. We conducted our experiments on an NVIDIA

A6000 graphical processing unit (GPU) machine.

4.15. ataza

Description: Team ataza proposes a low parameter efficient network, as shown in Fig. 15. Based on the observation that error in low light images mainly exist in the low-frequency region they decompose the image into high-frequency and low-frequency subbands using Discrete Wavelet Transform (DWT) whose utility for image processing has been well established [62]. Specifically, they choose HAAR wavelet [56] due to it's computational efficiency and excellent ability to detect edges [58]. The model consists of two branches one for high-frequency and the other for low-frequency features. This approach allows the model to focus on recovering low-frequency information while preserving high-frequency information that otherwise would have been lost in the deeper layers.

In the low-frequency branch, three Low-Frequency Blocks (LF Blocks) handle and extract low-frequency features. Subsequently, after each LF Block, a DWT block re-divides the output, channeling the high-frequency features to the high-frequency branch. Within the high-frequency branch, the existing high-frequency features are fused with those received via the DWT block from the low-frequency branch, before undergoing processing by the High-Frequency Block (HF Block). A total of four HF Blocks are employed in this process. This approach enables the model to preserve high-frequency features while concentrating on the recovery of low-frequency information. Given that the low-frequency subbands of the image have more errors, our approach involves making the LF Block deeper and more complex compared to the HF Block.

The outputs of the three LF Blocks are concatenated, while the outputs of the last three HF Blocks are also concatenated. Both sets of features are then fused and the final image generated. The model is trained using two loss functions: the L_1 loss and a frequency-domain-based loss $Loss_{FFT}$ derived from Fast Fourier Transform (FFT). $Loss_{FFT}$ is defined by Eq. (16), and the overall loss is determined by Eq. (17). Incorporating a frequency-based loss enhances model stability since the network is extracting features in the frequency domain, *i.e.* ,

$$Loss_{FFT} = \frac{1}{n}\sum_{i=1}^{n} ||FFT(I_g)| - |FFT(I_t)||, \tag{16}$$

$$Loss = Loss_{FFT} + 20 * Loss_{L_1}. \tag{17}$$

This approach enables the solution to possess only 387,414 parameters while still achieving competitive performance. It can process a 1024x1024 image in just 0.14s and a 512x512 image in 0.04s. The rapid speed, coupled with low complexity, renders it suitable for various real-world applications where a balance of performance and speed is crucial.

Implementation: The solution, developed in Python with the PyTorch framework, was trained on an Intel i7-8700 CPU @ 3.20GHz, 16GB RAM, and NVIDIA GeForce RTX 3070 graphics card. Data provided by the competition was exclusively used for training the model. The training dataset comprised 230 pairs of images, each sized 2992x2000 pixels. Out of these, 220 images were allocated for training, with the remaining 10 reserved for validation. To augment the dataset, non-overlapping patches of size 256x256 pixels were extracted from each image and used to train the model. Training lasted 70 epochs, employing the Cosine Annealing strategy with a cycle length of 10 epochs and an initial learning rate set at 0.0005. To train the model Adam optimizer, in conjunction with PyTorch's mixed precision feature was used and batch size was set to 8.

4.16. KLETech-CEVI_LowlightHypnotise

Description: The proposed MFNN framework includes three main modules: the hierarchical spatio-contextual (HSC) feature encoder, Global-Local Spatio-Contextual (GLSC) block, and hierarchical spatio-contextual (HSC) decoder, as shown in Fig. 16. Typically, low-light image enhancement networks employ feature scaling for varying the sizes of the receptive fields. The varying receptive fields facilitate learning of local-to-global variances in the features. With this motivation, we learn contextual information from multi-scale features while preserving high resolution spatial details. We achieve this via a hierarchical style encoder-decoder network with residual blocks as the backbone for learning. Given a input image x, the proposed multi-scale hierarchical encoder extracts shallow features in three distinct scales and is given as:

$$F_{si} = M_{Es}(x), \tag{18}$$

where F_{si} are the shallow features extracted at the i^{th} scale from the sampled space of input image x and, M_{Es} represents the hierarchical encoder at scale s. To learn the global-to-local representations from these shallow-level features, we propose a Global-Local Spatio-Contextual (GLSC) block, with residual blocks as the backbone. The learnt deep features are represented as:

$$D_{si} = \text{GLSC}_{si}(F_{si}), \tag{19}$$

where D_{si} is the deep feature at the i^{th} scale, F_{si} are the shallow features extracted at the i^{th} scale and, $GLSC_{si}$ represents residual blocks at respective scales. We decode the deep features obtained at various scales, with the proposed hierarchical decoder and is given by:

$$d_{si} = M_{dsi}(D_{si}), \tag{20}$$

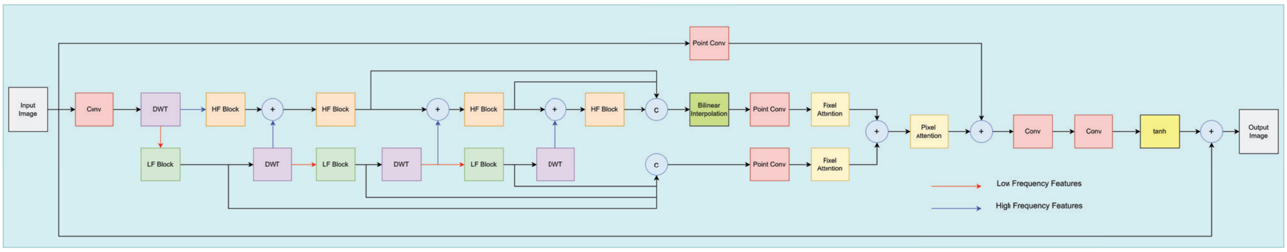

Figure 15. Overall framework our Team ataza's Frequency Guided Network

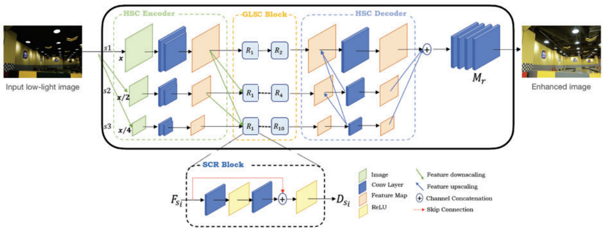

Figure 16. Overview of the proposed Multi-scale Feature FusionNet (MFNN). The encoder extracts features in three distinct scales, with information passed across hierarchies (green dashed box). Fine-grained global-local spatial and contextual information is learnt through the GLSC Block (orange dashed box). At decoder, information exchange occurs in reverse hierarchies (blue dashed box).

where d_{si} is the decoded feature at the i^{th} scale, and M_{dsi} represents the hierarchical decoder. The decoded features and upscaled features at each scale are passed to the reconstruction layers M_r to obtain the enhanced image $\hat{y}$. The upscaled features from each scale are stacked and represented as:

$$P = d_{s1} + d_{s2} + d_{s3}, \tag{21}$$

where d_{s1}, d_{s2}, and d_{s3} are decoded features at three distinct scales, P represents the final set of features passed to reconstruction layers to obtain the enhanced image $\hat{y}$:

$$\hat{y} = M_r(P), \tag{22}$$

where $\hat{y}$ is the enhanced image obtained from reconstruction layers M_r. We optimize the learning of MFNN with the proposed $\mathcal{L}_{MFNN}$ and is given as:

$$\mathcal{L}_{MFNN} = \alpha * L_1 + \beta * \mathcal{L}_{VGG} + \gamma * \mathcal{L}_{MSSSIM}, \tag{23}$$

where α, β, and γ are the weights. We experimentally set the weights to $\alpha = 0.5$, $\beta = 0.7$, and $\gamma = 0.5$. $\mathcal{L}_{MFNN}$ is a weighted combination of three distinct losses inspired from [25–27, 36]. L_1 loss to minimize error at pixel level, perceptual loss [43] to efficiently restore contextual information between the ground-truth image and the output image, multiscale structural dissimilarity loss to restore structural details. The aim here is to minimize the weighted combinational loss $\mathcal{L}_{MFNN}$ given as:

$$L(\theta) = \frac{1}{N}\sum_{i=1}^{N} \parallel MFNN(x_i - y_i) \parallel_{\mathcal{L}_{MFNN}}, \tag{24}$$

where θ denotes the learnable parameters of the proposed framework, N is the total number of training pairs, x and y are the input and output image respectively, and $MFNN(\cdot)$ is proposed framework for low-light image enhancement. **Implementation:** We train the proposed MFNN using Python (v3.8) coupled with PyTorch framework and conduct experiments on 2x NVIDIA RTX 3090 GPUs with AMD Ryzen ThreadRipper 3960X CPU. We use 16 residual blocks split into three layers of the hierarchy, and generate 256 feature maps for each scale. We train the proposed MFNN on dataset provided in the challenge along with LoL Dataset [71] with patches of size 600*400. During training, we use Adam optimizer with $\beta_1 = 0.9$, $\beta_2 = 0.999$, $\epsilon = 10e^{-8}$, and set the learning rate $lr = 0.0002$. We train the proposed MFNN for 1000 epochs. We optimize the learning with proposed $\mathcal{L}_{MFNN}$. During testing, we use full resolution images (2992 × 2000), on single RTX 3090 GPU. Average testing time for single image on full resolution is 0.53s on RTX 3090 GPU.

4.17. 221B

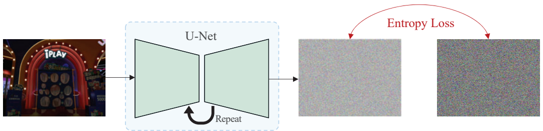

Figure 17. Overview of diffusion model training process with the differentiable spatial entropy loss proposed by the team 221B.

The organizer wants to highlight that this method has obtained the first place on the LPIPS ranking, with a score of 0.1084, outperforming the overall best-ranked work with a score of 0.1221.
Description: Most existing diffusion-based works [37] simply employ ℓ_1/ℓ_2 loss to train the noise prediction net-

work in a deterministic way, which always produces smooth intermediate noises (or states) in the reverse process. Although the perceptual quality can be improved with longer diffusion steps, it is reasonable to explore a perceptual-based loss function facilitate the training process. In this work, they propose to learn the network from a pure statistic perspective, that is, *directly learning distributions rather than pixel-by-pixel distances*. The core idea is the differentiable spatial entropy that drived from the kernel density estimation (KDE) and measures the spatial information of an image. Formally, following [3, 63], the two-dimensional KDE is defined as the probability of a specific intensity value i and its neighborhood j as:

$$\begin{aligned}\hat{f}_h(i,j) &= \frac{2}{Nh}\sum_{x\in X}\frac{1}{2}\mathbb{I}\left\{\frac{|x-i|}{h}<1\right\}\cdot\frac{1}{2}\mathbb{I}\left\{\frac{|\tilde{x}-j|}{h}<1\right\}\\ &= \frac{2}{Nh}\sum_{x\in X}\mathcal{K}_1(\frac{x-i}{h})\cdot\mathcal{K}_2(\frac{\tilde{x}-j}{h}),\end{aligned} \tag{25}$$

where $\mathcal{K}_1$ and $\mathcal{K}_2$ are arbitrary kernel functions (they can also be the same). To make use of the differentiable spatial KDE in image generation, this work considers to introduce the relative entropy (also called KL-divergence) to measure the distribution distance between the predicted image and ground truth. Let P and Q represent the ground truth's and prediction's probability distributions computed from Eq. (25), the spatial relative entropy is defined to be

$$H_s(P,Q) = D_{KL}(P||Q) = -\sum_{i=0}^{L}\sum_{j\in\Omega}p_{i,j}\log\frac{q_{i,j}}{p_{i,j}}. \tag{26}$$

Their diffusion model is built on the mean-reverting SDE [53, 54]. By optimizing the entropy-based distribution distance between predictions and ground truth states, their results have better visual qualities than that only using ℓ_1/ℓ_2 loss. Fig. 17 illustrates the overview of the proposed diffusion training process.

Implementation: This team use the provided low-light dataset but further split 10 image pairs for validation. The Refusion framework is used as the baseline and the team directly changed its loss funcion to the proposed differentiable spatial entropy. In training, all images are cropped with patch size 128 × 128, and the total training iteration is set to 500,000 with a batch 16. Following Refusion [54], this work use the AdamW [51] optimizer and the 'CosineDecay' scheduler with an initial learning rate 0.0001. And the diffusion steps are fixed to 100 in both training and testing.

4.18. KLETech-CEVI_Dark_Knights

Description: In accordance with the Retinex theory, there exists a relationship between the observed low-light image, denoted as y, and the desired clear image z, expressed as $y = z \otimes x$, where x signifies the illumination component. Typically, optimization efforts in low-light image enhancement primarily focus on refining the illumination component. To achieve enhanced output, one common approach involves removing the estimated illumination in accordance with the Retinex theory. Drawing inspiration from prior works on illumination optimization, particularly those employing a stage-wise approach, we propose a progressive perspective for modeling this task. Here, we introduce a mapping H_θ parameterized by θ to learn the illumination component, where each stage t (with $t = 0, ..., T-1$) consists of a basic unit represented as $u_t = H_\theta(x_t)$ and $x_{t+1} = x_t + u_t$, with $x_0 = y$. It's worth noting that we adopt a weight sharing mechanism across stages, utilizing the same architecture H and weights θ for each stage. Specifically, the parameterized operator H_θ effectively learns a simple residual representation u_t between the illumination and the observed low-light image. This process is motivated by the consensus that illumination and low-light observations exhibit similarities or linear connections in most areas.

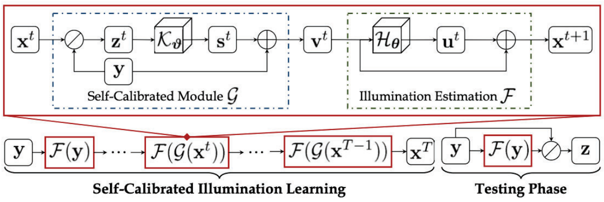
$\mathbf{x}^t$
$\mathbf{z}^t$
$\mathcal{K}_\vartheta$
$\mathbf{s}^t$
$\mathbf{v}^t$
$\mathcal{H}_\theta$
$\mathbf{u}^t$
$\mathbf{x}^{t+1}$
$\mathbf{y}$
Self-Calibrated Module $\mathcal{G}$
Illumination Estimation $\mathcal{F}$
$\mathbf{y}$
$\mathcal{F}(\mathbf{y})$
$\mathcal{F}(\mathcal{G}(\mathbf{x}^t))$
$\mathcal{F}(\mathcal{G}(\mathbf{x}^{T-1}))$
$\mathbf{x}^T$
$\mathbf{y}$
$\mathcal{F}(\mathbf{y})$
$\mathbf{z}$
Self-Calibrated Illumination Learning
Testing Phase

Figure 18. Framework of Self-Calibrated Illumination Module (Reproduced from [55]). We employ variant of this method for enhancement of low-light images with custom loss function.

We establish a module to ensure the convergence of results from each stage to a consistent state. Given that the input of each stage originates from the previous stage, and the initial input of the first stage is predetermined as the low-light observation, we propose to indirectly explore convergence behavior by bridging the input of each stage (excluding the first) with the low-light observation. To achieve this, we employ a self-calibrated module [55] denoted as s, which is added to the low-light observation to represent the disparity between the input of each stage and the initial stage. Specifically, the self-calibrated module, represented as $s = K_\theta(z)$, utilizes the parameterized operator K_θ with learnable parameters θ to generate $v = y + s$, where v_t denotes the converted input for each stage ($t \geq 1$). Consequently, the conversion for the basic unit in the t^{th} stage ($t \geq 1$) can be expressed as $F(x_t) \rightarrow F(G(x_t))$. This self-calibrated module effectively corrects the input of each stage by integrating physical principles, thereby indirectly influencing the output of each stage. In addition to this, we employ NIQE (Natural Image Quality Evaluator) [59] as a loss function. NIQE offers a valuable approach for improving perceptual quality. By utilizing NIQE as a metric to quantify the naturalness and perceptual fidelity of enhanced images, the training process aims to minimize the NIQE scores of the generated images. This strategy encourages the model to produce output images that closely resemble natural, high-quality images, enhancing their visual appeal and usability. By optimizing for lower NIQE scores, the model learns to prioritize perceptually pleasing enhancements, ultimately leading to outputs that are not only visually appealing but also retain important natural characteristics. Integrating NIQE as a loss function thus contributes to the development of low-light image enhancement techniques that align closely with human perception and preferences. NIQE as a loss function is given as:

$$L_{\text{NIQE}} = \frac{1}{N} \sum_{i=1}^{N} \text{NIQE}(F(G(x_{t,i}))), \tag{27}$$

where N is the number of samples, $x_{t,i}$ represents the input to the t-th stage for the i-th sample, $F(G(x_{t,i}))$ denotes the output of the t-th stage for the i-th sample after applying the self-calibrated module, and NIQE is the function that calculates the NIQE score for an image. Minimizing this loss function during training would encourage the model to produce output images with lower NIQE scores, indicating higher perceptual quality and naturalness. This would result in output images that are closer in quality to natural, high-quality images.

Implementation: We train the proposed method using Python (v3.8) coupled with PyTorch framework and conduct experiments on 2x NVIDIA RTX 3090 GPUs with AMD Ryzen ThreadRipper 3960X CPU. We use 16 residual blocks split into three layers of the hierarchy, and generate 256 feature maps for each scale. We train the proposed method on dataset provided in the challenge along with LoL Dataset [71] with images of size 2992*2000. During training, we use Adam optimizer with $\beta_1 = 0.9$, $\beta_2 = 0.999$, $\epsilon = 10e^{-8}$, and set the learning rate $lr = 0.0002$. We train the proposed method for 1000 epochs. During testing, we use full resolution images (2992 * 2000), on single RTX 3090 GPU. Average testing time for single image on full resolution is 0.53s on RTX 3090 GPU.

4.19. BFU-LL

Description: Diverging from the use of more complex, Transformer-based models for image restoration [30, 32], this team focuses on addressing low-light issues through the application of diffusion methods. They introduce a novel approach for enhancing low-light images proposed by [40], as illustrated in Fig. 19. The method first converting these images into the wavelet domain via 2D discrete wavelet transformation (DWT), iterated multiple times. This process yields an average coefficient and sets of high-frequency coefficients. By employing Haar wavelets [29], the method divides the input into four sub-bands, effectively capturing global information and sparse local details. This significantly reduces spatial dimensions while preserving essential image information. The team's wavelet-based diffusion model utilizes a forward diffusion process during the training phase and a denoising process across both training and inference phases. Moreover, they have developed a High-Frequency Restoration Module (HFRM) for the reconstruction of high-frequency details. Utilizing the U-Net architecture as the noise estimator network and implementing a fixed variance schedule, their method methodically transforms the input into corrupted noise data, subsequently employing Gaussian denoising transitions to achieve a clear and enhanced output.

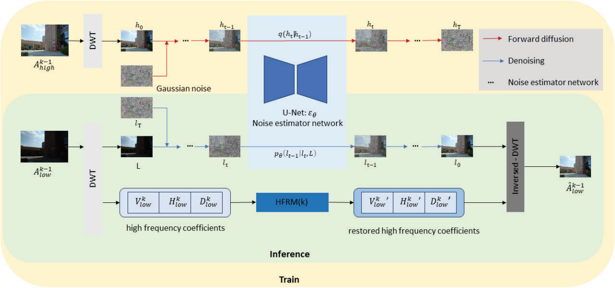

Figure 19. The network architecture of team BFU-LL.

Building on the methodologies described in previous studies [28, 76], this team design and adopt a hybrid loss function as follows:

$$\mathcal{L}_{\text{total}} = \mathcal{L}_{\text{smooth}} + \alpha\mathcal{L}_{\text{MS-SSIM}} + \beta\mathcal{L}_{\text{per}}, \tag{28}$$

where $\alpha = 0.01$, $\beta = 0.01$, and $\gamma = 0.005$ are the hyperparameters weighting each loss component.

Implementation: The implementation by this team is conducted using PyTorch. The proposed network effectively converges after undergoing training for 1×10^4 iterations on a system equipped with four NVIDIA RTX 1080Ti GPUs. For optimization, the Adam optimizer is employed. Considering the impact of the learning rate on experimental results [31], the initial learning rate is set to 1×10^{-4}. This learning rate decays by a factor of 0.8 after every 5×10^3 iterations. The team utilizes a batch size of 12 and a patch size of 256×256. The scale K for the wavelet transformation is set to 2.

4.20. SVNIT_NTNU

Description: In order to design low light image enhancement,we use multiple Retinex blocks and multiple channel attention in the proposed solution. The Fig. 20(a) de-

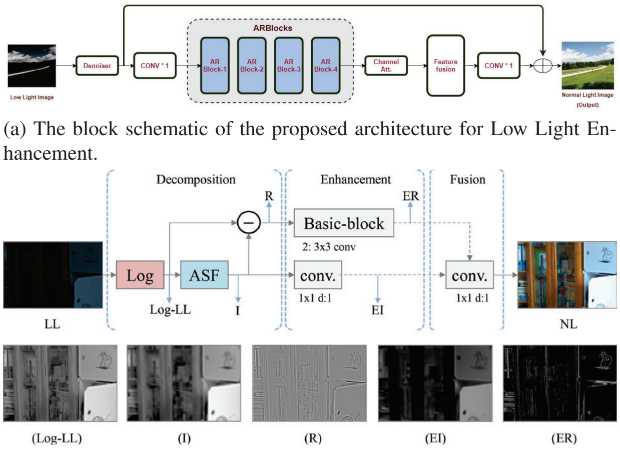

(a) The block schematic of the proposed architecture for Low Light Enhancement.

(b) The design of the ARblock used in the proposed model.

Figure 20. The architecture of the proposed model for Low Light Enhancement.

picts the proposed architecture for Low Light enhancement. The initial step involves feeding the low-light image into a denoiser module tailored to address the noise typical of low-exposure conditions. Subsequently, a shallow feature extraction process, achieved through a single convolutional operation, projects the denoised image into a feature space.

Following this, the image undergoes enhancement through multi-branch Adaptive Retinex (AR) Blocks operating at various scales. These blocks simultaneously enhance both broad and fine details within the image.

The shallow features and the enhanced results are then merged within a multiple channel attention module, which effectively extracts global and local features and combines them using a sigmoid function.

Lastly, the fused features are refined through another convolutional layer, culminating in the production of a clearer, brighter rendition of the original low-light image. Despite the addition of the channel attention module, which marginally increases parameter count, the overall network remains lightweight, owing to the efficiency achieved through the AR Blocks and denoiser modules.

The network incorporates multiple Adaptive Retinex Blocks (ARBlocks), which represent a novel extension of the Single Scale Retinex method in feature space [9]. At the core of each ARBlock lies an efficient illumination estimation function known as the Adaptive Surround Function (ASF) [82]. This function, akin to a general form of surround functions, is implemented using convolutional layers. The ARBlock serves a dual purpose, facilitating both illumination adjustment and reflectance enhancement within the image. Fig. 20 illustrates the architecture of the ARBlock, demonstrating its capability to enhance both low-frequency and high-frequency components of the image, respectively.

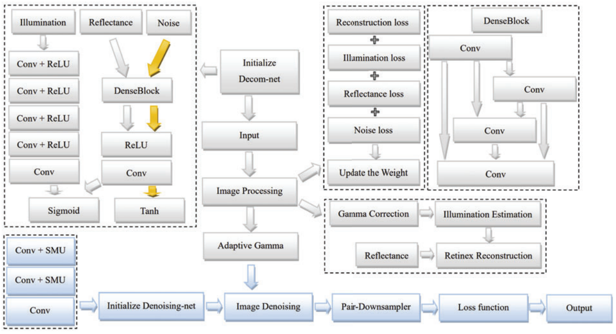

Figure 21. General method flow chart.

Implementation: The code is implemented using Pytorch library. The proposed network is trained using weighted combination of l_1, SSIM loss, and charbornnier loss with a learning rate of 1×10^{-4} which is decayed by 1×10^4 iterations and the same is optimized using Adam optimizer. The model is trained up to 1×10^5 iterations with a batch size of 4.

4.21. yanhailong

Description: We propose ZSRADNet: Zero-Shot Retinex Joint Adaptive-Illumination and Denoising for Underexposed Image Enhancement, which mainly considers underexposed images often suffer severe quality degradation. Many scenes exhibit issues related to occlusion and shadows, resulting in non-uniform illumination in the images. Most methods for restoring underexposed images rely on global enhancement, which can lead to excessive enhancement in areas that were originally well-lit. Both supervised and unsupervised learning approaches have limitations: either poor generalization or susceptibility to unstable training. To address these challenges, the proposed a Zero-Shot method that learns enhancement solely from test images. It consists of two main components: The Decomposition Network and The Denoising Network.

As shown in Fig. 21, inspired by [84], the Decomposition network employs a dual-branch structure to break down the input image into three components: Illumination, Reflection, and Noise. Initially, the input image passes through a simple four-layer CNN (Convolutional Neural Network) combined with ReLU (Rectified Linear Unit) activation and a Sigmoid function to obtain the illumination. Next, a designed DenseBlock layer, combined with ReLU and Convolution, generates the reflection (using Sigmoid activation) and the noise (using Tanh activation). DenseBlock can make better use of the feature information of the previous layer and help to improve feature reusability.

To achieve Zero-Shot enhancement, the proposed combines loss functions of Retinex reconstruction, Reflectance smoothness, and Illumination-guided noise estimation. By iteratively minimizing this combined loss function, the proposed effectively estimates the noise and restores the illumination. Additionally, the proposed introduces an adaptive gamma correction method that uses illumination as a measure of non-uniformly lit regions in the image. It brightens underexposed areas while leaving well-lit regions untouched. Our loss function consists of three parts:

$$L = L_{recon} + \lambda_{ref} \cdot L_{ref} + \lambda_{noise} \cdot L_{noise}, \tag{29}$$

where L_{recon}, L_{ref} and L_{noise} represent reconstruction loss, reflectance smoothness loss, and Illumination-guided noise loss respectively, and λ_{ref}, λ_{noise} represents corresponding weight factors.

The Denoising network generates a pair of noise maps [57] from a single noise image and utilizes these maps to train a simple three-layer network (CNN combined with SMU activation [6]). Specifically, the proposed begins by applying a down-sampling operator to decompose the output from the Decomposition network into a pair of downsampled images. One of these observations serves as the input value, while the other acts as the target. The proposed then employs regularization techniques during training to achieve effective denoising.

As a method specific to a single input image, it does not require any prior image samples or prior training models. The final enhanced results have advantages in the brightness and naturalness of non-uniform illumination images.

Implementation: The team uses Pytorch and the test device is the A6000 GPU. The illumination branch of the Decomposition network comprises a four-layer structure consisting of 3×3 Convolution followed by ReLU activation functions. On the other hand, the reflection and noise branches utilize a four-layer architecture of 3×3 Convolution with Denseblock, followed by ReLU activation functions, culminating in an additional layer of 3×3 Convolution. The network undergoes a total of 1000 iterations during training. In the Denoising network, two layers of 3×3 Convolution are employed, each followed by SMU activation, and ultimately connected to a final layer of 3×3 Convolution. The training process utilizes Mean Squared Error (MSE) loss is used for 2000 iterations. All the learning rates were 0.01; the optimizer uses Adam; without training, the input of a single image directly outputs the enhanced result.

4.22. Mishka

Description: As shown in Fig. 22, we employed the Retinexformer [8] model, a one-stage Retinex-based transformer, specifically designed for low-light image enhancement tasks. Our approach is distinguished by training the Retinexformer model directly on the dataset provided by the competition, demonstrating its adaptability and generalization capability across different datasets. This direct training method underscores the model's effectiveness and flexibility for specific low-light conditions. Our method maintains a moderate level of complexity throughout all stages, ensuring efficiency and effectiveness from data preprocessing to model training and final evaluation.

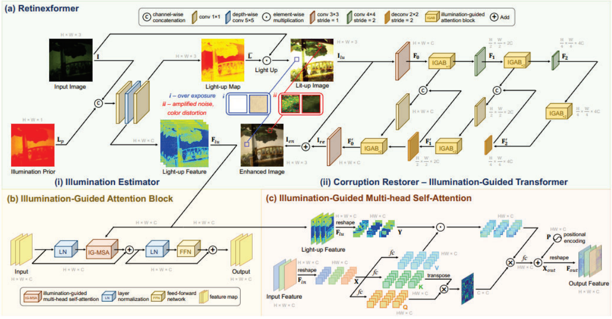

Figure 22. Illustrative diagram showing the application of Retinexformer for low-light enhancement.

Implementation: Our training configuration details various aspects of the model training process. We conducted a total of 300,000 iterations without a warm-up phase, and gradient clipping was employed to prevent gradient explosion. During training, we divided the 300,000 iterations into two cycles:

- The first cycle involved a fixed learning rate of $3e$-4 for the initial 92,000 iterations.
- The second cycle applied a cosine annealing strategy, decreasing the learning rate from $3e$-4 to $1e$-6 over the subsequent 208,000 iterations.

We also utilized mixed data augmentation techniques , and for the optimizer configuration, we chose the Adam optimizer with an initial learning rate of $2e$-4 and betas set to [0.9, 0.999]. Regarding the loss function, we employed the L_1 Loss, with a loss weight of 1 and reduction method set to mean.

Acknowledgements

This work was partially supported by the Humboldt Foundation. We thank the NTIRE 2024 sponsors: Meta Reality Labs, OPPO, KuaiShou, Huawei and University of Würzburg (Computer Vision Lab).

A. Teams and affiliations

NTIRE 2024 team

Title: NTIRE 2024 Low Light Enhancement Challenge
Members:
Xiaoning Liu[1] (liuxiaoning2016@sina.com),
Zongwei Wu[2] (zongwei.wu@uni-wuerzburg.de),
Ao Li[1] (aoli@std.uestc.edu.cn),
Florin Vasluianu[2] (florin-alexandru.vasluianu@uni-

wuerzburg.de),
Yulun Zhang[3] (yulun100@gmail.com),
Shuhang Gu[1] (shuhanggu@gmail.com),
Le Zhang[1] (lezhang@uestc.edu.cn),
Ce Zhu[1] (eczhu@uestc.edu.cn),
Radu Timofte[2,4] (radu.timofte@uni-wuerzburg.de)
Affiliations:
[1] University of Electronic Science and Technology of China, China
[2] Computer Vision Lab, University of Würzburg, Germany
[3] Shanghai Jiao Tong University, China
[4] Computer Vision Lab, ETH Zurich, Switzerland

SYSU-FVL-T2

Title: Scale-Robust Low-light Ultra-High-Definition Image Enhancement
Members:
Zhi Jin[1,2] (jinzh26@mail.sysu.edu.cn), Hongjun Wu[1], Chenxi Wang[1], Haitao Ling[1]
Affiliations:
[1] School of Intelligent Systems Engineering, Shenzhen Campus of Sun Yat-sen University, Shenzhen, Guangdong 518107, China
[2] Guangdong Provincial Key Laboratory of Fire Science and Technology, Guangzhou 510006, China

Retinexformer

Title: Retinexformer: One-stage Retinex-based Transformer for Low-light Image Enhancement
Members:
Yuanhao Cai[1] (caiyuanhao1998@gmail.com), Hao Bian[2], Yuxin Zheng[2], Jing Lin[2], Alan Yuille[1]
Affiliations:
[1] Johns Hopkins University
[2] Tsinghua University

DH-AISP

Title: Multi-scale feature fusion Low-light Image Enhancement
Members:
Ben Shao[1] (2830802483@qq.com), Jin Guo[1], Tianli Liu[1], Mohao Wu[1]
Affiliations:
[1] Zhejiang Dahua Technology Co.,Ltd.

NWPU-DiffLight

Title: DiffLight: Integrating Content and Detail for Low-light Image Enhancement
Members:
Yixu Feng[1] (yixu-nwpu@mail.nwpu.edu.cn), Shuo Hou[1], Haotian Lin[2], Yu Zhu[1], Peng Wu[1], Wei Dong[3], Jinqiu Sun[1], Yanning Zhang[1], Qingsen Yan[1]
Affiliations:
[1] School of Computer Science, Northwestern Polytechnical University, China
[2] School of Software, Northwestern Polytechnical University, China [3] School of Computer Science, Xi'an University of Architecture and Technology, China

GiantPandaCV

Title: UHDMamba: Towards Effective and Efficient State-Space Model for UHD Low-light Image Enhancement
Members:
Wenbin Zou[1] (alexzou14@foxmail.com), Weipeng Yang[1], Yunxiang Li[2], Qiaomu Wei[3], Tian Ye[4], Sixiang Chen[3,4]
Affiliations:
[1] South China University of Technology, China
[2] Fuzhou University, China
[3] Chengdu University of Information Technology, China
[4] Hong Kong University of Science and Technology (Guangzhou), China

LVGroup_HFUT

Title: Exploring the Application of NAFNet in Low Light Enhancement
Members:
Zhao Zhang[1] (cszzhang@gmail.com), Suiyi Zhao[1], Bo Wang[1], Yan Luo[1], Zhichao Zuo[1], Mingshen Wang[1], Junhu Wang[1], Yanyan Wei[1]
Affiliations:
[1] Hefei University of Technology, China

Try1try8

Title: Low Enhancement Model Ensemble of Multi-patch RetinexFormers
Members:
Xiaopeng Sun[1] (xpsun@stu.xidian.edu.cn), Yu Gao[1] , Jiancheng Huang[1]
Affiliations:
[1] Individual Researcher

Pixel_warrior

Title: MLP for Low-Light Image Enhancement
members:
Hongming Chen[1] (chenhongming@stu.sau.edu.cn), Xiang Chen[2]
Affiliations:
[1] Shenyang Aerospace University, China

[2] Nanjing University of Science and Technology, China

HuiT

Title: Enhanced Low-Light Imaging Method Based on Axis-Transformer
Members:
Hui Tang[1] (2639442956@qq.com), Yuanbin Chen[1], Yuanbo Zhou[1], Xinwei Dai[1], Xintao Qiu[1], Wei Deng[2], Qinquan Gao[1,2], Tong Tong[1,2]
Affiliations:
[1] Fuzhou University, Fuzhou, China
[2] Imperial Vision Technology, Fuzhou, China

X-LIME

Title: Supervised Deep Curve Estimation with Denoiser
Members:
Mingjia Li[1] (mingjiali@tju.edu.cn), Jin Hu[1], Xinyu He[1], Xiaojie Guo[1]
Affiliations:
[1] Tianjin University, China

Image Lab

Title: Enhancing Low-Light Images: A SCPA-Based Approach with RDCA-UNet Architecture
Members:
Sabarinathan[1] (sabarinathantce@gmail.com), K Uma[2], A Sasithradevi[3], B Sathya Bama[4], S. Mohamed Mansoor Roomi[4], V.Srivatsav[5]
Affiliations:
[1] Couger Inc,Japan
[2] Sasi Institute of Technology & Engineering, India
[3] Vellore Institute of Technology, India
[4] Thiagarajar college of engineering, India
[5] Coventry University, United Kingdom

dgzzqteam

Title: One-stage gatebased Framework
Members:
Jinjuan Wang (15600951607@163.com)[1], Long Sun[1], Qiuying Chen[1], Jiahong Shao[1], Yizhi Zhang[1]
Affiliations:
[1] Independent Researchers

Cidaut AI

Title: **InstructIR**: High-Quality Image Restoration Following Human Instructions
`https://github.com/mv-lab/InstructIR`
Members:
Marcos V. Conde[1,2] (marcos.conde@uni-wuerzburg.de), Daniel Feijoo[1], Juan C. Benito[1], Alvaro García[1]
Affiliations:
[1] Cidaut AI
[2] CVLab, University of Wuerzburg

OptDev

Title: Learning Optimized Low-Light Image Enhancement for Edge Vision Tasks
Members:
Jaeho Lee[1] (jaeho.lee@opt-ai.kr), Seongwan Kim[1], Sharif S M A[1], Nodirkhuja Khujaev[1], Roman Tsoy[1]
Affiliations:
[1] Opt-AI

ataza

Title: An Efficient Frequency Guided Image Enhancement Network for Low Light Image Enhancement and Shadow Removal
Members:
Ali Murtaza[1,2] (ali.murtaza.ali29@outlook.com), Uswah Khairuddin[1,2], Ahmad 'Athif Mohd Faudzi[2]
Affiliations:
[1] Malaysia-Japan International Institute of Technology (MJIIT), University Teknologi Malaysia, Kuala Lumpur, , Malaysia
[2] Center for Artificial Intelligence and Robotics (CAIRO), Universiti Teknologi Malaysia, Kuala Lumpur, Malaysia

KLETech-CEVI_LowlightHypnotise

Title: Hierarchical LightNet: Towards Low-Light Image Enhancement
Members:
Sampada Malagi[1,3] (sampadamalagi12@gmail.com), Amogh Joshi[1], Nikhil Akalwadi[1,3], Chaitra Desai[1,3], Ramesh Ashok Tabib[1,2], Uma Mudenagudi[1,2]
Affiliations:
[1] Center of Excellence in Visual Intelligence (CEVI), KLE Technological University, Hubballi, Karnataka, India
[2] School of Electronics and Communication Engineering, KLE Technological University, Hubballi, Karnataka, India
[3] School of Computer Science and Engineering, KLE Technological University, Hubballi, Karnataka, India

221B

Title: Equipping Diffusion Models with Differentiable Spatial Entropy for Low-Light Image Enhancement
Members:
Wenyi Lian[1] (shermanlian@163.com), Wenjing Lian[2]
Affiliations:

[1] Uppsala University
[2] Northeastern University

KLETech-CEVI_Dark_Knights

Title: KnightNet: Illumination Guided Low Light Image Enhancement Network ***Members:***
Jagadeesh Kalyanshetti[1,3] (01fe21bcs004@kletech.ac.in), Vijayalaxmi Ashok Aralikatti[1,3], Palani Yashaswini[1,2], Nitish Upasi[1], Dikshit Hegde[1], Ujwala Patil[1,2], Sujata C[1,3]
Affiliations:
[1] Center of Excellence in Visual Intelligence (CEVI), KLE Technological University, Hubballi, Karnataka, India
[2] School of Electronics and Communication Engineering, KLE Technological University, Hubballi, Karnataka, India
[3] School of Computer Science and Engineering, KLE Technological University, Hubballi, Karnataka, India

BFU-LL

Title: A Diffusion Model for Low-Light Enhancement
Members:
Xingzhuo Yan[1] (ayx1sgh@bosch.com), Wei Hao[2], Minghan Fu[3]
Affiliations:
[1] Bosch Investment Ltd.
[2] Fortinet, Inc.
[3] University of Saskatchewan

SVNIT_NTNU

Title: Retinex based Low Light Image Enhancement
Members:
Pooja choksy[1] (ds22ec003@eced.svnit.ac.in), Anjali Sarvaiya[1], Kishor Upla[1], Kiran Raja[2]

Affiliations:
[1] Sardar Vallabhbhai National Institute of Technology, India
[2] Norwegian University of Science and Technology, Norway

yanhailong

Title: ZSRADNet: Zero-Shot Retinex Joint Adaptive-Illumination and Denoising for Underexposed Image Enhancement
Members:
Hailong Yan (yhl00825@163.com),
Affiliations:
University of Electronic Science and Technology of China, China

Mishka

Title: Application and Adaptation of Retinexformer ***Members:***
Yunkai Zhang[1] (1585832651@qq.com), Baiang Li[1], Jingyi Zhang[1], Huan Zheng[2]
Affiliations:
[1] Hefei University of Technology, China
[2] University of Macau, China

References

[1] Cosmin Ancuti, Codruta O Ancuti, Florin-Alexandru Vasluianu, Radu Timofte, et al. NTIRE 2024 dense and non-homogeneous dehazing challenge report. In *Proceedings of the IEEE/CVF Conference on Computer Vision and Pattern Recognition (CVPR) Workshops*, 2024. 2

[2] Boaz Arad, Radu Timofte, Rony Yahel, Nimrod Morag, Amir Bernat, Yuanhao Cai, Jing Lin, Zudi Lin, Haoqian Wang, Yulun Zhang, et al. Ntire 2022 spectral recovery challenge and data set. In *Proceedings of the IEEE/CVF Conference on Computer Vision and Pattern Recognition*, pages 863–881, 2022. 5

[3] Mor Avi-Aharon, Assaf Arbelle, and Tammy Riklin Raviv. Differentiable histogram loss functions for intensity-based image-to-image translation. *IEEE Transactions on Pattern Analysis and Machine Intelligence*, 2023. 15

[4] Nikola Banić, Egor Ershov, Artyom Panshin, Oleg Karasev, Sergey Korchagin, Shepelev Lev, Alexandr Startsev, Daniil Vladimirov, Ekaterina Zaychenkova, Dmitrii R Iarchuk, Maria Efimova, Radu Timofte, Arseniy Terekhin, et al. NTIRE 2024 challenge on night photography rendering. In *Proceedings of the IEEE/CVF Conference on Computer Vision and Pattern Recognition (CVPR) Workshops*, 2024. 2

[5] Shiyin Wang Bin Xia, Yulun Zhang. Diffir: Efficient diffusion model for image restoration. In *ICCV*, 2023. 6, 7

[6] Koushik Biswas, Sandeep Kumar, Shilpak Banerjee, and Ashish Kumar Pandey. Smooth maximum unit: Smooth activation function for deep networks using smoothing maximum technique. In *Proceedings of the IEEE/CVF Conference on Computer Vision and Pattern Recognition*, pages 794–803, 2022. 18

[7] Vladimir Bychkovsky, Sylvain Paris, Eric Chan, and Frédo Durand. Learning photographic global tonal adjustment with a database of input/output image pairs. In *CVPR 2011*, pages 97–104. IEEE, 2011. 2

[8] Yuanhao Cai, Hao Bian, Jing Lin, Haoqian Wang, Radu Timofte, and Yulun Zhang. Retinexformer: One-stage retinex-based transformer for low-light image enhancement. In *Proceedings of the IEEE/CVF International Conference on Computer Vision*, pages 12504–12513, 2023. 1, 2, 3, 4, 5, 18

[9] Yuanhao Cai, Hao Bian, Jing Lin, Haoqian Wang, Radu Timofte, and Yulun Zhang. Retinexformer: One-stage retinex-based transformer for low-light image enhancement. In *Proceedings of the IEEE/CVF International Conference on Computer Vision*, pages 12504–12513, 2023. 17

[10] Yuanhao Cai, Jing Lin, Xiaowan Hu, Haoqian Wang, Xin Yuan, Yulun Zhang, Radu Timofte, and Luc Van Gool.

Coarse-to-fine sparse transformer for hyperspectral image reconstruction. In *ECCV*, 2022. 4

[11] Yuanhao Cai, Jing Lin, Xiaowan Hu, Haoqian Wang, Xin Yuan, Yulun Zhang, Radu Timofte, and Luc Van Gool. Mask-guided spectral-wise transformer for efficient hyperspectral image reconstruction. In *CVPR*, 2022. 5

[12] Yuanhao Cai, Jing Lin, Zudi Lin, Haoqian Wang, Yulun Zhang, Hanspeter Pfister, Radu Timofte, and Luc Van Gool. Mst++: Multi-stage spectral-wise transformer for efficient spectral reconstruction. In *CVPRW*, 2022. 5

[13] Yuanhao Cai, Jing Lin, Haoqian Wang, Xin Yuan, Henghui Ding, Yulun Zhang, Radu Timofte, and Luc Van Gool. Degradation-aware unfolding half-shuffle transformer for spectral compressive imaging. In *NeurIPS*, 2022. 4

[14] Yuanhao Cai, Jiahao Wang, Alan Yuille, Zongwei Zhou, and Angtian Wang. Structure-aware sparse-view x-ray 3d reconstruction. In *CVPR*, 2024.

[15] Yuanhao Cai, Zhicheng Wang, Zhengxiong Luo, Binyi Yin, Angang Du, Haoqian Wang, Xinyu Zhou, Erjin Zhou, Xiangyu Zhang, and Jian Sun. Learning delicate local representations for multi-person pose estimation. In *ECCV*, 2020.

[16] Yuanhao Cai, Yuxin Zheng, Jing Lin, Xin Yuan, Yulun Zhang, and Haoqian Wang. Binarized spectral compressive imaging. In *NeurIPS*, 2023. 4

[17] Nicolas Chahine, Marcos V. Conde, Sira Ferradans, Radu Timofte, et al. Deep portrait quality assessment. a NTIRE 2024 challenge survey. In *Proceedings of the IEEE/CVF Conference on Computer Vision and Pattern Recognition (CVPR) Workshops*, 2024. 2

[18] Liangyu Chen, Xiaojie Chu, Xiangyu Zhang, and Jian Sun. Simple baselines for image restoration. In *European conference on computer vision*, pages 17–33, 2022. 8

[19] Liangyu Chen, Xiaojie Chu, Xiangyu Zhang, and Jian Sun. Simple baselines for image restoration. In Shai Avidan, Gabriel J. Brostow, Moustapha Cissé, Giovanni Maria Farinella, and Tal Hassner, editors, *Computer Vision - ECCV 2022 - 17th European Conference, Tel Aviv, Israel, October 23-27, 2022, Proceedings, Part VII*, volume 13667 of *Lecture Notes in Computer Science*, pages 17–33. Springer, 2022. 11

[20] Zheng Chen, Zongwei WU, Eduard Sebastian Zamfir, Kai Zhang, Yulun Zhang, Radu Timofte, Xiaokang Yang, et al. NTIRE 2024 challenge on image super-resolution (×4): Methods and results. In *Proceedings of the IEEE/CVF Conference on Computer Vision and Pattern Recognition (CVPR) Workshops*, 2024. 2

[21] Xiaojie Chu, Liangyu Chen, Chengpeng Chen, and Xin Lu. Improving image restoration by revisiting global information aggregation. In Shai Avidan, Gabriel J. Brostow, Moustapha Cissé, Giovanni Maria Farinella, and Tal Hassner, editors, *Computer Vision - ECCV 2022 - 17th European Conference, Tel Aviv, Israel, October 23-27, 2022, Proceedings, Part VII*, volume 13667 of *Lecture Notes in Computer Science*, pages 53–71. Springer, 2022. 11

[22] M.V. Conde, F. Vasluianu, S. Nathan, and R. Timofte. Real-time under-display cameras image restoration and hdr on mobile devices. In *Computer Vision – ECCV 2022 Workshops*, volume 13802 of *Lecture Notes in Computer Science*. Springer, Cham, 2023. 11

[23] Marcos V Conde, Gregor Geigle, and Radu Timofte. High-quality image restoration following human instructions. *arXiv preprint arXiv:2401.16468*, 2024. 3, 12

[24] Marcos V. Conde, Florin-Alexandru Vasluianu, Radu Timofte, et al. Deep raw image super-resolution. a NTIRE 2024 challenge survey. In *Proceedings of the IEEE/CVF Conference on Computer Vision and Pattern Recognition (CVPR) Workshops*, 2024. 2

[25] Chaitra Desai, Nikhil Akalwadi, Amogh Joshi, Sampada Malagi, Chinmayee Mandi, Ramesh Ashok Tabib, Ujwala Patil, and Uma Mudenagudi. Lightnet: Generative model for enhancement of low-light images. In *Proceedings of the IEEE/CVF International Conference on Computer Vision*, pages 2231–2240, 2023. 14

[26] Chaitra Desai, Sujay Benur, Ramesh Ashok Tabib, Ujwala Patil, and Uma Mudenagudi. Depthcue: Restoration of underwater images using monocular depth as a clue. In *Proceedings of the IEEE/CVF Winter Conference on Applications of Computer Vision (WACV) Workshops*, pages 196–205, January 2023.

[27] Chaitra Desai, Badduri Sai Sudheer Reddy, Ramesh Ashok Tabib, Ujwala Patil, and Uma Mudenagudi. Aquagan: Restoration of underwater images. In *Proceedings of the IEEE/CVF Conference on Computer Vision and Pattern Recognition (CVPR) Workshops*, pages 296–304, June 2022. 14

[28] Minghan Fu, Yanhua Duan, Zhaoping Cheng, Wenjian Qin, Ying Wang, Dong Liang, and Zhanli Hu. Total-body low-dose ct image denoising using a prior knowledge transfer technique with a contrastive regularization mechanism. *Medical Physics*, 50(5):2971–2984, 2023. 16

[29] Minghan Fu, Huan Liu, Yankun Yu, Jun Chen, and Keyan Wang. Dw-gan: A discrete wavelet transform gan for nonhomogeneous dehazing. In *Proceedings of the IEEE/CVF conference on computer vision and pattern recognition*, pages 203–212, 2021. 16

[30] Minghan Fu, Meiyun Wang, Yaping Wu, Na Zhang, Yongfeng Yang, Haining Wang, Yun Zhou, Yue Shang, Fang-Xiang Wu, Hairong Zheng, et al. A two-branch neural network for short-axis pet image quality enhancement. *IEEE Journal of Biomedical and Health Informatics*, 2023. 16

[31] Minghan Fu and Fang-Xiang Wu. Qlabgrad: A hyperparameter-free and convergence-guaranteed scheme for deep learning. In *Proceedings of the AAAI Conference on Artificial Intelligence*, volume 38, pages 12072–12081, 2024. 16

[32] Minghan Fu, Na Zhang, Zhenxing Huang, Chao Zhou, Xu Zhang, Jianmin Yuan, Qiang He, Yongfeng Yang, Hairong Zheng, Dong Liang, et al. Oif-net: An optical flow registration-based pet/mr cross-modal interactive fusion network for low-count brain pet image denoising. *IEEE Transactions on Medical Imaging*, 2023. 16

[33] Albert Gu and Tri Dao. Mamba: Linear-time sequence modeling with selective state spaces. *arXiv preprint arXiv:2312.00752*, 2023. 7

[34] Chunle Guo, Chongyi Li, Jichang Guo, Chen Change Loy, Junhui Hou, Sam Kwong, and Runmin Cong. Zero-reference deep curve estimation for low-light image enhancement. In *Proceedings of the IEEE/CVF conference on computer vi-*

sion and pattern recognition, pages 1780–1789, 2020. 1, 10, 12

[35] Chunle Guo, Chongyi Li, Jichang Guo, Chen Change Loy, Junhui Hou, Sam Kwong, and Runmin Cong. Zero-reference deep curve estimation for low-light image enhancement. In *2020 IEEE/CVF Conference on Computer Vision and Pattern Recognition, CVPR 2020, Seattle, WA, USA, June 13-19, 2020*, pages 1777–1786. Computer Vision Foundation / IEEE, 2020. 11

[36] Dikshit Hegde, Tejas Anvekar, Ramesh Ashok Tabib, and Uma Mudengudi. Da-ae: Disparity-alleviation auto-encoder towards categorization of heritage images for aggrandized 3d reconstruction. In *Proceedings of the IEEE/CVF Conference on Computer Vision and Pattern Recognition*, pages 5093–5100, 2022. 14

[37] Jonathan Ho, Ajay Jain, and Pieter Abbeel. Denoising diffusion probabilistic models. In *Advances in neural information processing systems*, volume 33, pages 6840–6851, 2020. 14

[38] Jinhui Hou, Zhiyu Zhu, Junhui Hou, Hui Liu, Huanqiang Zeng, and Hui Yuan. Global structure-aware diffusion process for low-light image enhancement. *Advances in Neural Information Processing Systems*, 36, 2024. 2

[39] Hai Jiang, Ao Luo, Haoqiang Fan, Songchen Han, and Shuaicheng Liu. Low-light image enhancement with wavelet-based diffusion models. *ACM Transactions on Graphics (TOG)*, 42(6):1–14, 2023. 1, 2

[40] Hai Jiang, Ao Luo, Haoqiang Fan, Songchen Han, and Shuaicheng Liu. Low-light image enhancement with wavelet-based diffusion models. *ACM Transactions on Graphics (TOG)*, 42(6):1–14, 2023. 16

[41] Diederik P. Kingma and Jimmy Lei Ba. Adam: A method for stochastic optimization. In *ICLR*, 2015. 4, 5, 7, 8

[42] Wei-Sheng Lai, Jia-Bin Huang, Narendra Ahuja, and Ming-Hsuan Yang. Fast and accurate image super-resolution with deep laplacian pyramid networks. *IEEE transactions on pattern analysis and machine intelligence*, 41(11):2599–2613, 2018. 4

[43] Christian Ledig, Lucas Theis, Ferenc Husz'ar, Jose Caballero, Andrew Cunningham, Alejandro Acosta, Andrew Aitken, Alykhan Tejani, Johannes Totz, Zehan Wang, et al. Photo-realistic single image super-resolution using a generative adversarial network. In *Proceedings of the IEEE conference on computer vision and pattern recognition*, pages 4681–4690, 2017. 14

[44] Xin Li, Kun Yuan, Yajing Pei, Yiting Lu, Ming Sun, Chao Zhou, Zhibo Chen, Radu Timofte, et al. NTIRE 2024 challenge on short-form UGC video quality assessment: Methods and results. In *Proceedings of the IEEE/CVF Conference on Computer Vision and Pattern Recognition (CVPR) Workshops*, 2024. 2

[45] Jie Liang, Qiaosi Yi, Shuaizheng Liu, Lingchen Sun, Rongyuan Wu, Xindong Zhang, Hui Zeng, Radu Timofte, Lei Zhang, et al. NTIRE 2024 restore any image model (RAIM) in the wild challenge. In *Proceedings of the IEEE/CVF Conference on Computer Vision and Pattern Recognition (CVPR) Workshops*, 2024. 2

[46] R. Liu et al. An intriguing failing of convolutional neural networks and the coordconv solution. *Advances in Neural Information Processing Systems*, 2018:9605–9616, 2018. 11

[47] Risheng Liu, Long Ma, Jiaao Zhang, Xin Fan, and Zhongxuan Luo. Retinex-inspired unrolling with cooperative prior architecture search for low-light image enhancement. In *Proceedings of the IEEE/CVF conference on computer vision and pattern recognition*, pages 10561–10570, 2021. 1, 2

[48] Xiaohong Liu, Xiongkuo Min, Guangtao Zhai, Chunyi Li, Tengchuan Kou, Wei Sun, Haoning Wu, Yixuan Gao, Yuqin Cao, Zicheng Zhang, Xiele Wu, Radu Timofte, et al. NTIRE 2024 quality assessment of AI-generated content challenge. In *Proceedings of the IEEE/CVF Conference on Computer Vision and Pattern Recognition (CVPR) Workshops*, 2024. 2

[49] Xiaoning Liu, Zongwei Wu, Ao Li, Florin-Alexandru Vasluianu, Yulun Zhang, Shuhang Gu, Le Zhang, Ce Zhu, Radu Timofte, et al. NTIRE 2024 challenge on low light image enhancement: Methods and results. In *Proceedings of the IEEE/CVF Conference on Computer Vision and Pattern Recognition (CVPR) Workshops*, 2024. 2

[50] Yue Liu, Yunjie Tian, Yuzhong Zhao, Hongtian Yu, Lingxi Xie, Yaowei Wang, Qixiang Ye, and Yunfan Liu. Vmamba: Visual state space model. *arXiv preprint arXiv:2401.10166*, 2024. 7

[51] Ilya Loshchilov and Frank Hutter. Decoupled weight decay regularization. *arXiv preprint arXiv:1711.05101*, 2017. 15

[52] Ilya Loshchilov and Frank Hutter. Sgdr: Stochastic gradient descent with warm restarts. In *ICLR*, 2017. 4, 5, 7

[53] Ziwei Luo, Fredrik K Gustafsson, Zheng Zhao, Jens Sjölund, and Thomas B Schön. Image restoration with mean-reverting stochastic differential equations. *arXiv preprint arXiv:2301.11699*, 2023. 15

[54] Ziwei Luo, Fredrik K Gustafsson, Zheng Zhao, Jens Sjölund, and Thomas B Schön. Refusion: Enabling large-size realistic image restoration with latent-space diffusion models. In *Proceedings of the IEEE/CVF conference on computer vision and pattern recognition*, pages 1680–1691, 2023. 15

[55] Long Ma, Tengyu Ma, Risheng Liu, Xin Fan, and Zhongxuan Luo. Toward fast, flexible, and robust low-light image enhancement. In *Proceedings of the IEEE/CVF conference on computer vision and pattern recognition*, pages 5637–5646, 2022. 1, 2, 12, 15

[56] S G Mallat. A theory for multiresolution signal decomposition: the wavelet representation. *IEEE Transactions on Pattern Analysis and Machine Intelligence*, 11(7):674–693, 1987. 13

[57] Youssef Mansour and Reinhard Heckel. Zero-shot noise2noise: Efficient image denoising without any data. In *Proceedings of the IEEE/CVF Conference on Computer Vision and Pattern Recognition*, pages 14018–14027, 2023. 18

[58] John Mashford, Mike Rahilly, Brad Lane, Donavan Marney, and Stewart Burn. Edge detection in pipe images using classification of haar wavelet transforms. *Applied Artificial Intelligence*, 28(7):675–689, Aug. 2014. 13

[59] Anish Mittal, Rajiv Soundararajan, and Alan C Bovik. Making a "completely blind" image quality analyzer. *IEEE Signal processing letters*, 20(3):209–212, 2012. 3, 15

[60] D. Nathan, K. Uma, D. S. Vinothini, B. S. Bama, and S. M. M. Roomi. Light weight residual dense attention net for spectral reconstruction from rgb images. *arXiv preprint arXiv:2004.06930*, 2020. 11

[61] S. Nathan and P. Kansal. End-to-end depth-guided relighting

using lightweight deep learning-based method. *J. Imaging*, 9:175, 2023. 11

[62] Hyun-Wook Park and Hyung-Sun Kim. Motion estimation using low-band-shift method for wavelet-based moving-picture coding. *IEEE Transactions on Image Processing*, 9(4):577–587, Apr. 2000. 13

[63] Emanuel Parzen. On estimation of a probability density function and mode. *The annals of mathematical statistics*, 33(3):1065–1076, 1962. 15

[64] Bin Ren, Yawei Li, Nancy Mehta, Radu Timofte, et al. The ninth NTIRE 2024 efficient super-resolution challenge report. In *Proceedings of the IEEE/CVF Conference on Computer Vision and Pattern Recognition (CVPR) Workshops*, 2024. 2

[65] Chen Change Loy Shangchen Zhou, Chongyi Li. Lednet: Joint low-light enhancement and deblurring in the dark. In *ECCV*, 2022. 6, 7

[66] Karen Simonyan and Andrew Zisserman. Very deep convolutional networks for large-scale image recognition. *arXiv preprint arXiv:1409.1556*, 2014. 4

[67] Florin-Alexandru Vasluianu, Tim Seizinger, Zhuyun Zhou, Zongwei Wu, Cailian Chen, Radu Timofte, et al. NTIRE 2024 image shadow removal challenge report. In *Proceedings of the IEEE/CVF Conference on Computer Vision and Pattern Recognition (CVPR) Workshops*, 2024. 2

[68] Longguang Wang, Yulan Guo, Juncheng Li, Hongda Liu, Yang Zhao, Yingqian Wang, Zhi Jin, Shuhang Gu, Radu Timofte, et al. NTIRE 2024 challenge on stereo image super-resolution: Methods and results. In *Proceedings of the IEEE/CVF Conference on Computer Vision and Pattern Recognition (CVPR) Workshops*, 2024. 2

[69] Tao Wang, Kaihao Zhang, Tianrun Shen, Wenhan Luo, Bjorn Stenger, and Tong Lu. Ultra-high-definition low-light image enhancement: A benchmark and transformer-based method. In *Proceedings of the AAAI Conference on Artificial Intelligence*, volume 37, pages 2654–2662, 2023. 2, 9, 10

[70] Yingqian Wang, Zhengyu Liang, Qianyu Chen, Longguang Wang, Jungang Yang, Radu Timofte, Yulan Guo, et al. NTIRE 2024 challenge on light field image super-resolution: Methods and results. In *Proceedings of the IEEE/CVF Conference on Computer Vision and Pattern Recognition (CVPR) Workshops*, 2024. 2

[71] Chen Wei, Wenjing Wang, Wenhan Yang, and Jiaying Liu. Deep retinex decomposition for low-light enhancement. In *British Machine Vison Conference*, 2018. 2, 12, 14, 16

[72] Xiaogang Xu, Ruixing Wang, Chi-Wing Fu, and Jiaya Jia. Snr-aware low-light image enhancement. In *Proceedings of the IEEE/CVF conference on computer vision and pattern recognition*, pages 17714–17724, 2022. 1, 2

[73] Ren Yang, Radu Timofte, et al. NTIRE 2024 challenge on blind enhancement of compressed image: Methods and results. In *Proceedings of the IEEE/CVF Conference on Computer Vision and Pattern Recognition (CVPR) Workshops*, 2024. 2

[74] Shuzhou Yang, Moxuan Ding, Yanmin Wu, Zihan Li, and Jian Zhang. Implicit neural representation for cooperative low-light image enhancement. In *Proceedings of the IEEE/CVF International Conference on Computer Vision*, pages 12918–12927, 2023. 2

[75] Xin Yu, Peng Dai, Wenbo Li, Lan Ma, Jiajun Shen, Jia Li, and Xiaojuan Qi. Towards efficient and scale-robust ultra-high-definition image demoiréing. In *European Conference on Computer Vision*, pages 646–662. Springer, 2022. 3

[76] Yankun Yu, Huan Liu, Minghan Fu, Jun Chen, Xiyao Wang, and Keyan Wang. A two-branch neural network for non-homogeneous dehazing via ensemble learning. In *Proceedings of the IEEE/CVF conference on computer vision and pattern recognition*, pages 193–202, 2021. 16

[77] Pierluigi Zama Ramirez, Fabio Tosi, Luigi Di Stefano, Radu Timofte, Alex Costanzino, Matteo Poggi, et al. NTIRE 2024 challenge on HR depth from images of specular and transparent surfaces. In *Proceedings of the IEEE/CVF Conference on Computer Vision and Pattern Recognition (CVPR) Workshops*, 2024. 2

[78] Syed Waqas Zamir, Aditya Arora, Salman Khan, Munawar Hayat, Fahad Shahbaz Khan, Ming-Hsuan Yang, and Ling Shao. Learning enriched features for real image restoration and enhancement. In *Computer Vision–ECCV 2020: 16th European Conference, Glasgow, UK, August 23–28, 2020, Proceedings, Part XXV 16*, pages 492–511. Springer, 2020. 1, 2

[79] Syed Waqas Zamir, Aditya Arora, Salman Khan, Munawar Hayat, Fahad Shahbaz Khan, Ming-Hsuan Yang, and Ling Shao. Learning enriched features for fast image restoration and enhancement. *IEEE transactions on pattern analysis and machine intelligence*, 45(2):1934–1948, 2022. 4

[80] Richard Zhang, Phillip Isola, Alexei A Efros, Eli Shechtman, and Oliver Wang. The unreasonable effectiveness of deep features as a perceptual metric. In *Proceedings of the IEEE conference on computer vision and pattern recognition*, pages 586–595, 2018. 2

[81] Zhilu Zhang, Shuohao Zhang, Renlong Wu, Wangmeng Zuo, Radu Timofte, et al. NTIRE 2024 challenge on bracketing image restoration and enhancement: Datasets, methods and results. In *Proceedings of the IEEE/CVF Conference on Computer Vision and Pattern Recognition (CVPR) Workshops*, 2024. 2

[82] Fei Zhou, Xin Sun, Junyu Dong, and Xiao Xiang Zhu. Surroundnet: Towards effective low-light image enhancement. *Pattern Recognition*, 141:109602, 2023. 17

[83] Han Zhou, Wei Dong, Yangyi Liu, and Jun Chen. Breaking through the haze: An advanced non-homogeneous dehazing method based on fast fourier convolution and convnext. In *Proceedings of the IEEE/CVF Conference on Computer Vision and Pattern Recognition*, pages 1894–1903, 2023. 6

[84] Anqi Zhu, Lin Zhang, Ying Shen, Yong Ma, Shengjie Zhao, and Yicong Zhou. Zero-shot restoration of underexposed images via robust retinex decomposition. In *2020 IEEE International Conference on Multimedia and Expo (ICME)*, pages 1–6. IEEE, 2020. 17

[85] Wenbin Zou, Tian Ye, Weixin Zheng, Yunchen Zhang, Liang Chen, and Yi Wu. Self-calibrated efficient transformer for lightweight super-resolution. In *Proceedings of the IEEE/CVF Conference on Computer Vision and Pattern Recognition*, pages 930–939, 2022. 11